SLAC Proposal No. E-127

STUDY OF EVENTS WITH DIRECT e^+e^- PAIRS IN HADRON COLLISIONS AT 10 AND 16 GeV/c

W. Dunwoodie, S. Durkin, M. Ferro-Luzzi†, T.H. Fieguth, M. Gilchriese, A. Honma, D. Hutchinson, W.B. Johnson, P. Kunz, T. Lasinski, D.W.G.S. Leith, J. Malos, W. T. Meyer, B. Ratcliff, P. Schacht, S. Shapiro, R. Stroynowski, S.H. Williams

Stanford Linear Accelerator Center
Stanford University, Stanford, California

G. Fox, R. Gomes, M. Marshall, J. Pine, J. Scheid

California Institute of Technology
Pasadena, California

B. Barnett, D. Blockus, C.Y. Chien, L. Madansky, A. Pevsner, C. Woody, R. Zdanis

John Hopkins University
Baltimore, Maryland

R. K. Carnegie

Carleton University
Ottawa, Ontario, Canada

August 1976

† On leave of absence from CERN, Geneva, Switzerland

I. INTRODUCTION

The discovery of direct lepton production in hadronic collisions (1) has aroused considerable interest during recent years. Direct production is taken to mean leptons originating from processes other than Dalitz decays of π^o or η, external γ-conversions or the decays of particles stable against the strong interactions.

At high energy the rate of production of direct leptons is found to be about 10^{-4} that of pion production (2). This rate is possibly even higher at small transverse momenta (3). A rough visualisation of the lepton/pion ratio in the x-p_T plane is attempted in fig. 1. Recent results from Fermilab experiments (4) indicate that most of the observed signal is due to lepton pair production. At low energies the experimental results are contradictory. Re-analyses of old experiments (5) yield no evidence of direct leptons at 12 and 19 GeV/c in pp collisions. Together with a rather low value of the μ/π ratio at 28 and 35 GeV/c (6), these results would indicate the onset of a threshold for direct lepton production in the neighbourhood of 20 GeV/c. Preliminary results from the Pennsylvania-Stony Brook experiment (7) indicate, however, that the e/π ratio is $\sim 10^{-4}$ and possibly even higher for small p_T in the energy range from 10 to 24 GeV. On the other hand, no experimental information is available on direct electron pair production in this energy range.

The high rate of lepton production cannot be accounted for entirely by the decay of known particles (8). An additional source is required and this indicates the existence of new phenomena such as the Drell-Yan mechanism, the production and semi-leptonic decay of charmed particles, the production and conversion of virtual photons, etc. A single electron in the final state is possible in events with charmed particles or heavy leptons. Various models give different predictions concerning the yield, the pair mass spectrum and

the correlations between produced leptons and accompanying hadrons.

In order to study these problems we propose an experiment to measure events with e^+e^- pair production by hadrons using a large solid angle detector (LASS) which has good acceptance in the $p_T - p_L$ plane. The experiment will try to answer the following questions:

a) are all direct electrons produced in pairs or are there also single electrons?

b) what is the mass spectrum of direct electron pairs for $M_{e^+e^-} > 0.1$ GeV and what is its dependence on p_T and p_L?

c) what are the characteristics of the hadronic system accompanying the direct electrons (i.e. multiplicity, K/π ratio, resonance production, correlations, etc.)?

The experiment will also study the energy and projectile dependence of direct electron pair production by collecting π^-p, K^-p and $\bar{p}p$ data at 10 GeV/c as well as π^-p data at 16 GeV/c.

II. SET-UP

The apparatus consists of the Large Acceptance Solenoid Spectrometer (LASS) with the addition of total absorption shower counters placed in front of the dipole magnet (SC_1) and behind the downstream Cerenkov counter (SC_2). A plan view of the set-up is shown in fig. 2. A complete description of LASS is given in the Appendix. The Appendix includes a full discussion of the beam, the solenoid and dipole magnets and the various detectors used. It also contains a description of the data acquisition system, including on-line monitoring facilities and a discussion of the off-line analysis program.

In order to adapt LASS to the electron experiment the following changes have been made:

1) The last spark chamber of the solenoid package has been removed and the multicell Cerenkov counter C_1 has been extended by 0.6 m inside the solenoid. This counter, filled with air at atmospheric pressure, allows e/π separation below 5.8 GeV/c laboratory momentum. The prototype of one cell of the C_1 counter was tested in the 2.5 and 5.0 GeV/c RF separated beams and found to have hadron rejection of $2 \cdot 10^{-4}$ with a 90% electron detection efficiency.

2) In the region between the magnets we have placed two large-area magnetostrictive spark chambers sandwiching a proportional wire hodoscope (vertical wires with 4 mm spacing). Following is the wall of shower counters SC_1 described below. A CD-spark chamber-PWC-plug package is mounted in front of the entrance to the dipole magnet.

3) A shower counter wall SC_2 has been placed behind C_2 to detect small p_T forward going electrons.

Shower Counters

The geometrical configuration of the shower counter wall SC_1 between the two magnets is shown in fig. 3. It consists of 10 total absorption counters constructed by SLAC Group E for experiment E97 (16 radiation lengths of lead interspaced by scintillator) and 6 shower counters constructed by the Cal-Tech group. Each Cal-Tech counter consists of 3 layers of lucite separated by a total of 4 radiation lengths of lead. They are used in two arrays separated by three radiation lengths of lead plate with independent pulse height read-out from each array. In this configuration the first array serves as pre-radiator for the second array. In order to distinguish between signals from electrons and from photons, the active area of each of the shower counters in the SC_1 wall was covered by thin scintillation counters.

The downstream shower counter SC_2 consists of four packages 20" x 40" of 6 layers of scintillator separated by a total of 10 radiation lengths of lead and iron.

All three types of shower counter were tested for hadron rejection in the 2.5 and 5.0 GeV/c beams. With a 90% electron detection efficiency the hadron rejection was found to be:

a) for the Group E counters in SC_1: better than 10^{-2},

b) for the two arrays of Cal-Tech counters in SC_1: $2 \cdot 10^{-2}$,

c) for the SC_2 counters: $6 \cdot 10^{-2}$.

Electron Identification

Electron identification is provided by the coincidence of the signals from either

1) the Cerenkov counter C_1 and a shower counter in SC_1 with its corresponding gamma-veto scintillation counter

or

2) the Cerenkov counter C_1 and the SC_2 shower counter.

This identification is used both in the event trigger and in identifying the electron tracks among those reconstructed in the off-line analysis program.

The combined hadron rejection for particles in the momentum range $1.0 \leq p_{LAB} \leq 5.8$ GeV/c which pass through C_1 and SC_1 is estimated to be better than 4.10^{-6}; that for particles passing through C_1 and SC_2 is better than $1.2 \cdot 10^{-5}$.

Beam

We intend to use RF separated beams of π^- at 16 GeV/c and $\bar{p}$, K^- and π^- at 10 GeV/c. The electron contamination is negligible in all cases. The beam line has two Cerenkov counters for tagging purposes.

The multiwire proportional chambers in the beam line provide resolution

of the beam of $\pm 0.3\%$, the divergence ± 0.5 mrad and the spread in space at the interaction point is ± 1mm. A detailed description of the beam line and its recent modifications can be found in the appendix and in ref. (9).

III. GEOMETRICAL ACCEPTANCE

While the geometrical acceptance for normal tracks in LASS is close to 4π, the acceptance for electron pairs is limited by the identification requirements and the dynamics of their production. In order to estimate it we have used two different models for pair production:

1) The constituent annihilation Drell-Yan model modified by M. Duong-Van (10).

2) A model in which all the electrons come from the decay of an object of mass M which has the same momentum spectrum as pions produced in $\pi^- p$ collisions at 16 GeV/c.

The resulting acceptances are shown as a function of $M_{e^+e^-}$ in fig. 4.

The kinematical region covered by the acceptance slowly varies with the mass of the electron pair. It covers the full p_T range for $x > -0.2$. The contours of acceptance in the x vs p_T plane calculated in the framework of model 2 are plotted in fig. 5 for $M_{e^+e^-} = 0.5$ GeV.

For each mass of the e^+e^- pair the spectrometer provides a uniform acceptance of the decay angular distribution in the range $-0.95 < \cos\theta < +0.95$. The effective mass resolution as a function of mass is given in Table I.

IV. BACKGROUND

The most important contributions to the background come from Dalitz decay of π^o and external γ-conversion near the interaction vertex. To study this background we used 20,000 bubble chamber events of the reaction $\pi^+ p \rightarrow$ anything at 22 GeV (11). Assuming that the production of non-leading pions, i.e. π^-'s

is similar to that of π^o's, we used the momentum vectors of the π^- on an event by event basis to represent the production of π^o's. In a Monte Carlo program we simulated Dalitz decays and γ conversions using the corresponding momentum and angular distribution of resulting electrons (12) and branching ratios. The conversion point of the γ's inside the solenoid magnet was generated according to the probability distribution due to the radiation length of the material traversed (i.e. target, spark chambers, etc.). Most of this background will be rejected by the analysis whenever both tracks of the e^+e^- pair are measured. The procedure is as follows.

In event reconstruction we assume that we lose a track if:

(i) the momentum is below 100 MeV,

(ii) the particle stops in the target,

(iii) there are less then 3 measured points available from the spark and proportional chambers.

Additionally we assume a vertex resolution given by

(i) $\sigma(z) = 1$ cm (the z-axis is parallel to the beam axis)

(ii) $\sigma(x) = \sigma(y) = 0.2$ cm

The mass resolution being about 8 MeV in the region $0.5 < M_{e^+e^-} < 1.0$ GeV, a cut at 0.1 GeV in the e^+e^- mass and at 3σ in the distance between the event vertex and the electron pair vertex will eliminate both the external conversions and Dalitz decays.

The background which remains after this analysis, expressed as a fraction of the direct electron pair signal for $M_{e^+e^-} > 0.1$ GeV, is listed below:

π^o decays	0.30
Hadron misidentification	$< 10^{-7}$
$\eta \to \gamma\gamma$	$3 \cdot 10^{-4}$
$\eta \to \pi\, e^+e^-$, $\pi\pi\, e^+e^-$	10^{-2}
$K^\pm \to e^\pm\, \pi^o\, \nu$	10^{-4}
$K_L^o \to e\, \pi\, \nu$	$1.8 \cdot 10^{-4}$

Most of this background is concentrated in the region of small e^+e^- effective mass, and for $M_{e^+e^-} > 300$ MeV the background reduces to 2% of the signal.

V. RATES

A) Event Rates

We assume that the inclusive cross section for electron production is

$$\sigma(e^\pm) = 10^{-4} \cdot \sigma_{incl}\ (\pi^\pm) = 4\ \mu b.$$

At 180 pulses per second and with a flux yielding $\sim$ 1 interaction per pulse (i.e. $\sim$ 10 particles/spill for our liquid hydrogen target) there are 26 interactions/μb/hour. The number of events we shall obtain per hour of running is then given by

$$26\ \text{events}/\mu b \cdot 4\ \mu b \cdot \text{Acceptance} \cdot \text{Efficiency}.$$

The acceptance of the apparatus is defined by the acceptance in the low mass range of the electron pair and we take it to be about 10% (see fig. 4)*. The efficiency of the LASS spectrometer and its software is arbitrarily taken to be 75%. The resulting estimated rate is 7.5 direct electron pairs per hour.

B) Trigger Rates

On the basis of the bubble chamber data we have also estimated the trigger rates as follows:

---

* This number takes account of the fact that we cannot equip all of the active area in the SC_1 wall and C_1 counter in the forthcoming accelerator period.

a) the trigger rate due to γ conversion with both electrons identified and both having energy $E > 0.5$ GeV is 0.26% of the total cross section. This small number is due to the fact that we demand that particles miss the innermost cell of C_1 counter, which is equivalent to a minimum transverse momentum cut and eliminates most of the background.

b) the trigger rate due to two fast pions ($p_{LAB} > 5.8$ GeV/c) giving a signal in C_1 and simulating electrons in the shower counters. There are 3% of the events with two fast pions which fall within the range of acceptance of the shower counters. Assuming conservatively that the hadron rejection in the shower counter is 6.10^{-2}, the trigger rate due to such fast pions is $3\% \times (6.10^{-2})^2 = 1.08 \cdot 10^{-4}$.

c) the trigger rate due to a single electron from π^o decay and a fast pion simulating an electron in the shower counter is 0.35%.

The total trigger rate for pairs is then a) + b) + c) + signal = 0.62% of the total cross section. Assuming a repetition rate of 180 pulses/sec and a flux corresponding to 1 interaction/pulse, this rate is $\sim$ 4000 triggers/hour. This low trigger rate will allow for simultaneous collection of data with a single electron trigger i.e. requiring only one identified electron in C_1 and shower counters. These events will be used to estimate limits on single electron production.

We intend to run the equivalent of 300 hours at 180 pps with π^- at 16 GeV/c and then for 300 hours of $\bar{p}$, 300 hours of K^- and 100 hours of π^- at 10 GeV/c.

VII. ANALYSIS

The structure of a complete package of software programs is ready, hence we expect to complete the analysis of the data one year after the end of the data taking. The computing needs for the analysis are estimated as $\sim$ 1000 hours of 370/168 time. An additional $\sim$ 500 hours will be needed for pre-selection

of events, Monte Carlo studies and the analysis of samples of single electron triggers.

VIII. SUMMARY

We propose a measurement of direct e^+e^- pair production in hadronic collisions using the Large Aperture Solenoid Spectrometer (LASS). The purpose is to study at low energy the anomalous lepton/pion ratio observed in earlier experiments. The experiment will study events with e^+e^- pairs in π^-p interactions at 16 GeV/c and $\bar{p}p$, K^-p and π^-p interactions at 10 GeV/c. The equivalent of 1000 hours at 180 pps will yield $\sim$ 7000 events with direct pairs with good mass resolution. The residual background due to Dalitz decay and external γ conversion is estimated to be $\sim$ 30% of the signal in the low mass region ($M_{e^+e^-} < 0.3$ GeV) and $\sim$ 2% for $M_{e^+e^-} > 0.3$ GeV. Simultaneous measurements of the associated charged hadrons will yield information on the origin of direct leptons and their production mechanism. We are ready to run in the coming accelerator cycle (October-November 1976).

As a by-product of the experiment we will be able to study Dalitz decays of η and ω produced in hadron collisions. We also expect several thousand events with fully identified π^o i.e. both γ's converted and measured.

REFERENCES

1. J. P. Boymond et al., Phys. Rev. Letters 33 (1974) 112.
   J. A. Appel et al., Ph . Rev. Letters 33 (1974) 722.
   F. W. Büsser et al., Phys. Letters 53 B (1974) 212.

2. L. M. Lederman, Lepton Production in Hadron Collisions. Proceedings of the 1975 International Symposium on Lepton and Photon Interactions, Stanford 1975.

3. L. Baum et al., Phys. Letters 60 B (1976) 485.

4. K. J. Anderson et al. "The contribution of muon pairs to the yield of single prompt muons." Paper submitted to the XVIII Conf. in High Energy Physics, Tbilisi, 1976.
   H. Kasha et al., Phys. Rev. Letters 36 (1976) 1007.

5. R. C. Lamb et al., Phys. Rev. Letters 15 (1965) 800.
   K. Winter, Phys. Letters 57 B (1975) 479.

6. L. B. Leipuner et al., Phys. Rev. Letters 34 (1975) 103.
   V. V. Abramov et al., Direct muon production in proton-nuclear collisions at 70, 50 and 35 GeV, Serpukhov preprint.

7. E. W. Beier et al., Anamalous production of direct electrons at 10, 15 and 24 GeV/c. University of Pennsylvania report.

8. M. Bourquin and J.-M. Gaillard, Phys. Letters 59 B (1975) 191 and CERN preprint "A simple phenomenological description of hadron production."

9. F. Winkelman, Design and Operation of SLAC Beamline 20-21-22, SLAC Report 160.

10. M. Duong-Van, Phys. Letters 60 B (1976) 287.

11. We are grateful to H. Gordon (BNL) for providing the data.

12. N. Kroll and W. Wada, Phys. Rev. 98 (1955) 1355.
    Y. Tsai, Rev. of Mod. Phys. 46 (1974) 815.

TABLE I

e^+e^- Pair Mass Resolution (σ)

$M_{e^+e^-}$ (GeV)	0.5 - 1.0	1.0 - 2.0	2.0 -3.0	3.0 - 4.0
σ (MeV)	8	12	14	24

Figure Captions

1. Artist's impression of the lepton/pion ratio in the (x, p_T) plane.

2. Plan view of the experimental set-up. Solid lines represent spark chambers, dashed lines represent proportional wire chambers, dotted lines proportional wire hodoscopes, and dot-dashed lines indicate scintillation counters.

3. Geometrical configuration of the shower counter wall SC_1 in the x-y plane. Numbers 1 to 10 denote group E counters and 11 to 13 the Cal-Tech counters.

4. Acceptance for electron pairs as a function of M (e^+e^-) for the two models described in the text.

5. Constant acceptance curves (in %) for electron pairs in the (x, p_T), plane for $M(e^+e^-) = 0.5$ GeV.

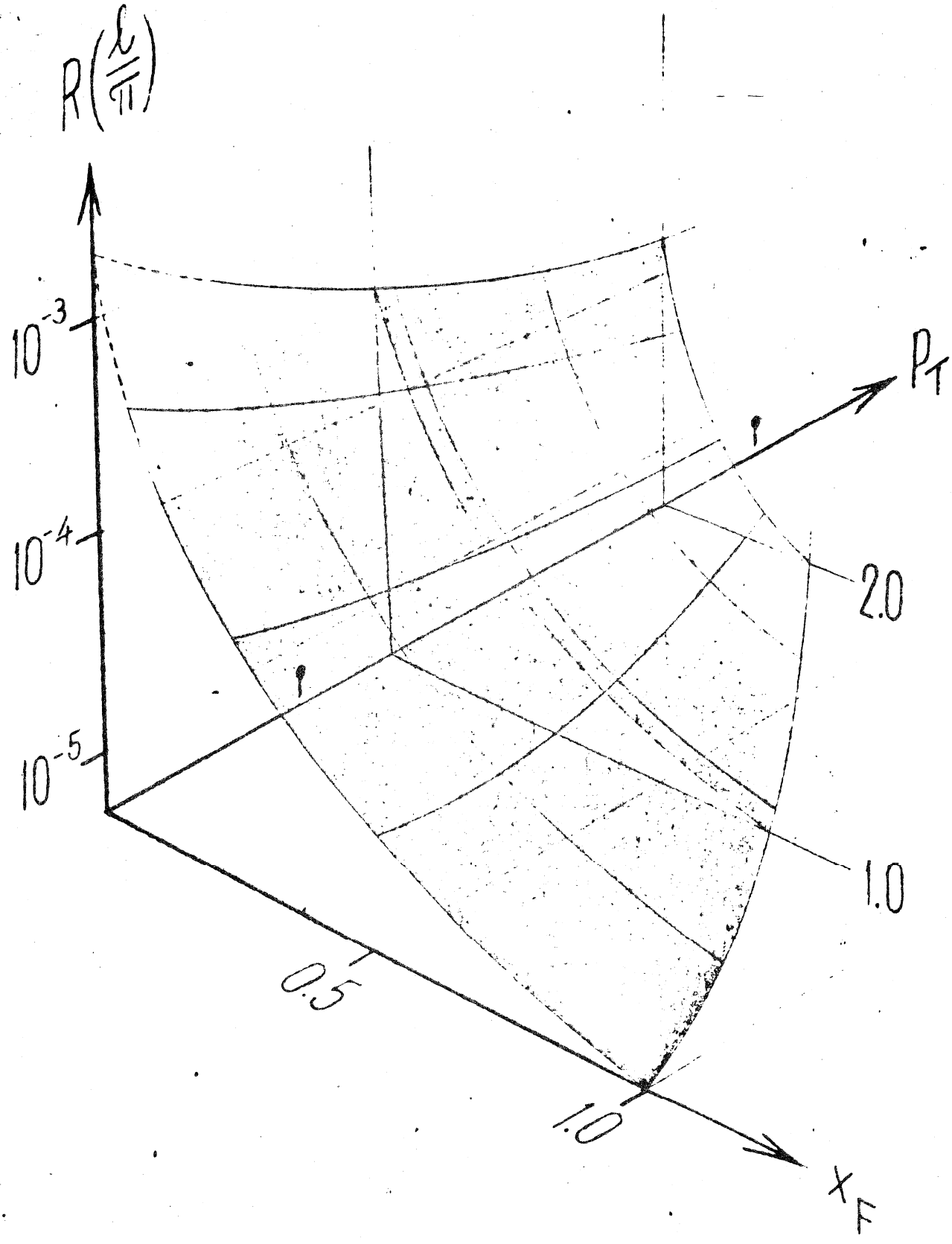

FIG. 1

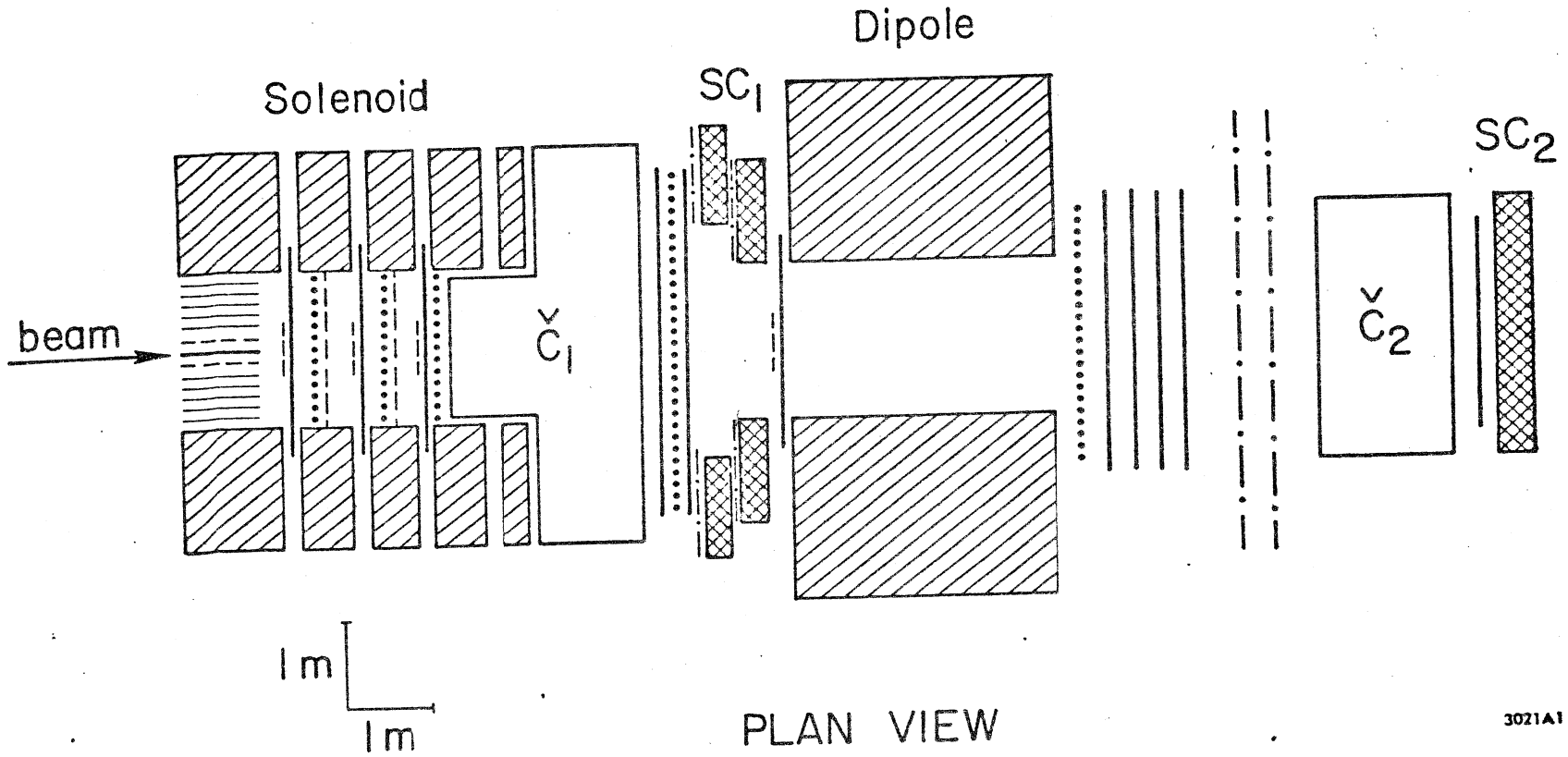

FIG. 2

SHOWER COUNTERS SC_1

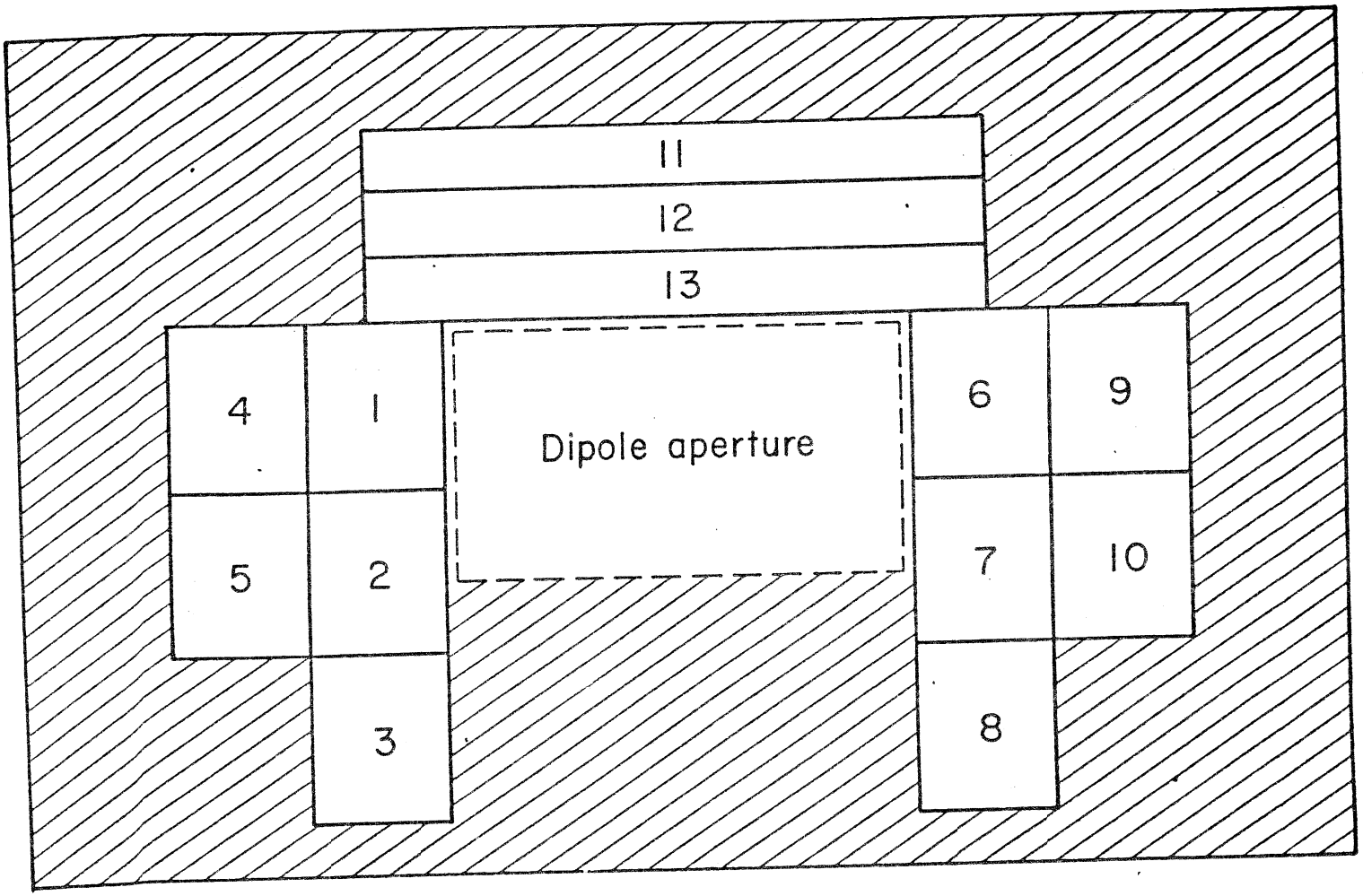

FIG. 3

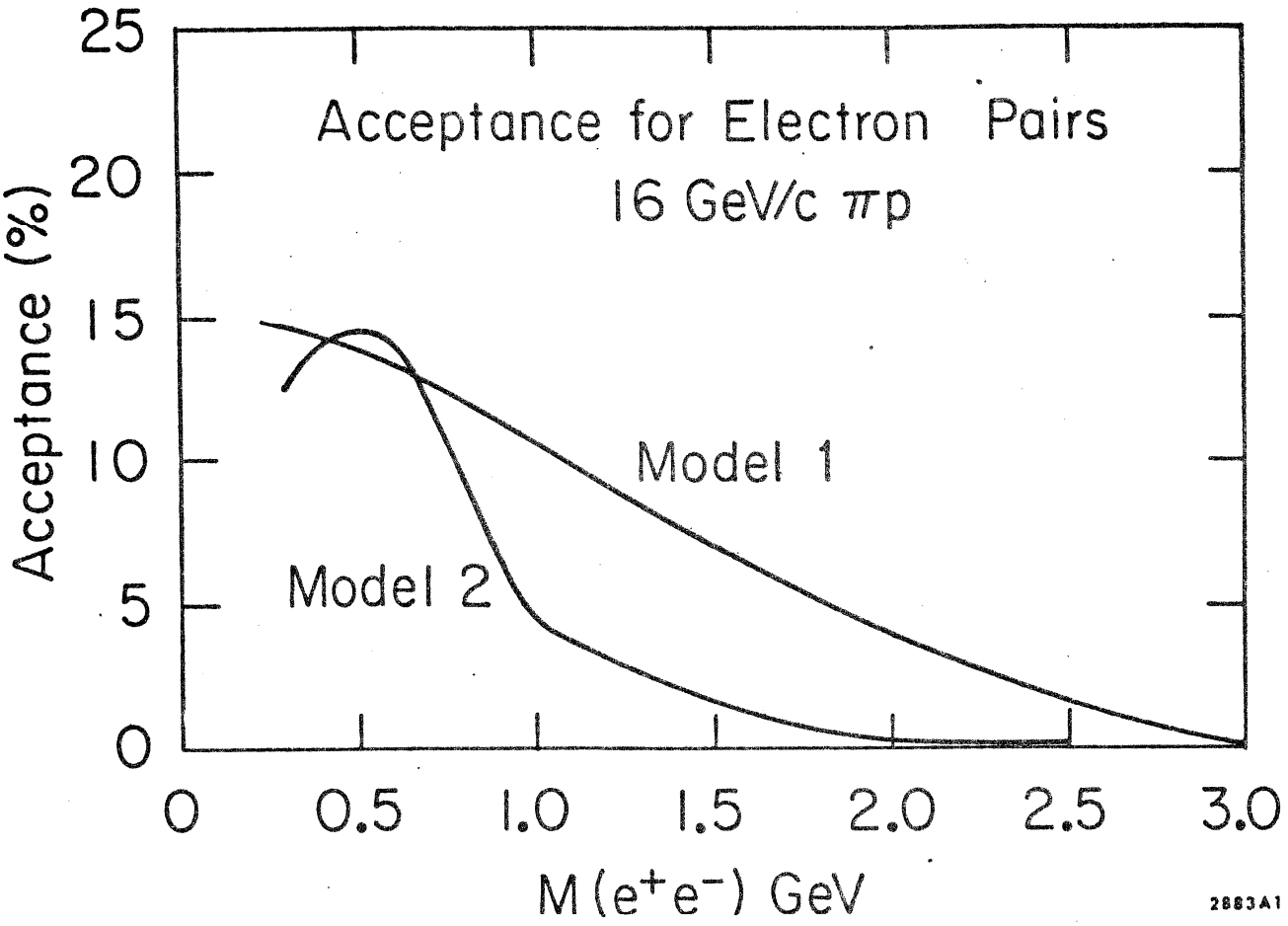
Acceptance for Electron Pairs
16 GeV/c πp
Model 1
Model 2
Acceptance (%)
25
20
15
10
5
0
0
0.5
1.0
1.5
2.0
2.5
3.0
M(e+e−) GeV
2883A1

FIG. 4

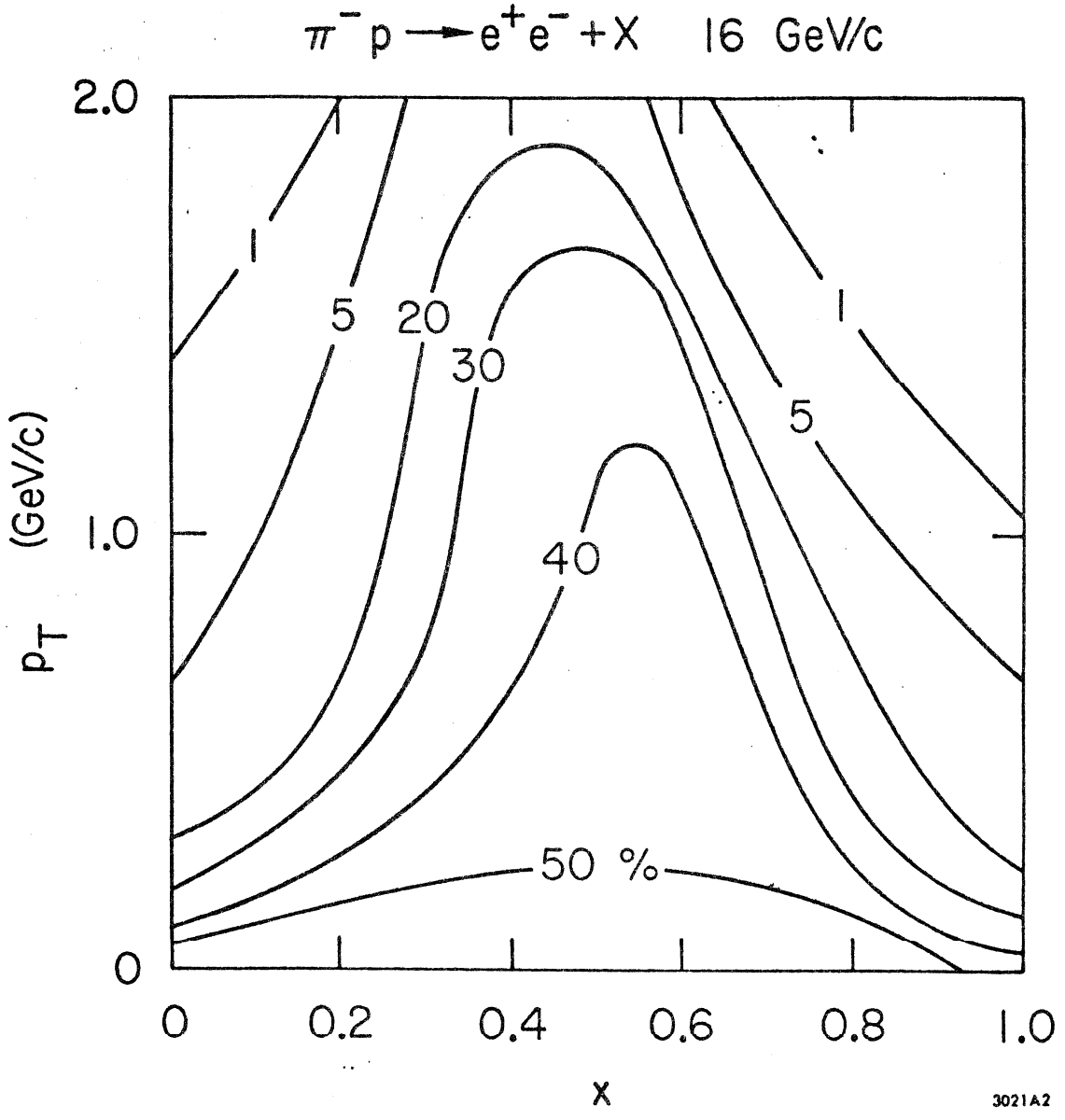
$\pi^- p \rightarrow e^+ e^- + X$ 16 GeV/c
2.0
1.0
0
p_T (GeV/c)
0
0.2
0.4
0.6
0.8
1.0
X
1
5
20
30
40
50 %
1
5
3021A2

FIG. 5

Appendix

The LASS Spectrometer

A. Introduction

LASS consists of two large magnets and the associated detectors as shown in Figure 1. The first magnet is a superconducting solenoid of 23 25kG maximum field with the field direction horizontal, parallel to the beam line, followed by a 16kG field dipole with vertical field direction. The solenoid is effective in measuring the interaction products which have large production angles and relatively low momentum. High energy secondaries, tending to stay close to the beam line, are not measured well in the solenoid, but will pass through the dipole for measurement there. Table 1 contains the parameters of these magnets.

The liquid hydrogen target is placed at the up beam end of the solenoid. Wide angle secondaries from the target are detected by CP1, a cylindrical proportional wire chamber surrounding the target and CS1-CS5, cylindrical wire spark chambers also concentric with the target. The forward going particles are detected by plane wire spark chambers CD1-CD4, which have 10 in. x 10 in. proportional wire chamber plugs, P1-P4, attached to measure particles near the beam, where the rate is highest. There is a full bore proportional wire chamber, PWC1.5 placed midway between CD1 and CD2. Identical plane wire spark chambers, CD5-CD7, detect particles in the region between solenoid and dipole. Following the dipole are magneto-strictive read out wire spark chambers MS1-MS5. $\check{C}1$ and $\check{C}2$ are used to identify K,p from π,μ,e, and scintillation counter hodoscopes HA and HB are used to aid in triggering the spark chamber and in track finding in event reconstruction.

Figure 2 shows the placement of the spectrometer in the LASS Building, No. 121. A crane of 7.5 ton capacity covers the building to within a

few feet of each wall. The building is heated and air conditioned to stabilize the temperature.

Section B of this appendix will discuss the beam, Section C the LH target and the detectors, Section D proposed trigger schemes, Section E data collection and recording and Section F the event reconstruction.

B. Beam

Beam line 20-21-22 originates in End Station B as a single line (20) and then divides at a dipole into beams 21 (left bend) and 22 (right bend). Beam 21 is the LASS beam, beam 22 now partly dismantled, served the 1971-73 Group B spectrometer and its design was the basis for the new beam 21, built in the summer of 1973. Table 2 contains the beam line parameters. SLAC publication 160 by Frederick Winkelmann, Design and Operation of SLAC Beamline 20-21-22, contains detailed and extensive information on beams 20-22, which is useful to LASS users as the instrumentation of beam 20 is retained for LASS, and the two beam line rf separators are located in beam 20. The tuning procedure for these rf separators is given step by step in SLAC-160.

Figure 3 shows beam line 20-21. The basic instrumentation is a scintillation counter coincidence, $S_1 \cdot S_2$, at F2 (the first triple focus), the p hodoscope at F3 where there is momentum dispersion of 0.5 in/per % $\Delta P/P$, the θ,ϕ hodoscope which is a scintillation counter hodoscope, actually giving x,y information, from which the beam particle incident angles can be derived by comparison with a second detector, the beam proportional chamber, placed just before the target. There are two threshold Cerenkov counters, K and π detectors, also placed just before the target. The final focus is at the downstream end of the target and is the second triple focus.

S_1 and S_2 have 1/4" scintillators. The p hodoscope is formed of six scintillators, 1/8 in. thick, which are 50% overlapped to form eleven momentum bins, each bin .25 in. wide representing ± .25% in momentum resolution.

The π Cerenkov counter is 5 m. long and can be filled to 40 psia (usually run with H_2 gas as radiator), counting the π's only. The K Cerenkov is 1 m. long and filled with Freon, counting K's and π's. The above detectors are also described in SLAC-160.

The θ-φ hodoscope has been rebuilt of thinner scintillator, now 1/16 in. thick. There are two arrays of 12 counters, placed edge to edge, each 0.5" wide. One array is formed of vertical counters, the other of horizontal, to give ± .25" resolution in both x and y. This hodoscope is located 40 ft. upstream of the beam proportional chamber. The maximum angular resolution is ± .25 in./480 in., or ± 0.5 mrad. (Actual angular resolution is limited by small angle scattering in the $\check{C}$ counters to approximately 1 mrad). The small angle scattering in 50 cm of the target, at 7.5 GeV/c beam momentum, is 0.5 mrad.

The beam porportional chamber is placed just before the LH target. There are 8 planes of proportional wires in the beam chamber system divided into two groups separated by one meter. Each plane consists of 64-20 micron diameter gold plated tungsten wires placed 1 mm apart. The signal plane is 4 mm from either of the high voltage cathodes. There are 5 grounded guard wires having increasing diameters on either side of the signal plane to prevent breakdown. This chamber design has been tested in the previous experiment and found to be quite stable and satisfactory. The upstream group of four planes is arranged so that we measure x,y,e,p coordinates (horizontal, vertical, and ± 45° planes). The downstream group has 2 sets of x,y planes one offset from the other by $\frac{1}{2}$ mm. This

arrangement should give us the position of a particle entering the solenoid to better than $\frac{1}{2}$ mm, and its direction to better than 1 milliradian.

Control of the beam line magnets will be done by the YARDMUX system presently under development by the EFD Electronics Group. An independent computer, to be located in LASS control room, will scan and control magnet power supplies and a link to the LASS computer system is planned so that eventually the beam line will be under experimental program control.

C-1. Target

The Liquid Hydrogen target is 36" long by 2" in diameter. The target cell is fabricated as two concentric mylar cylinders, the inner cylinder having .001 to .002" wall thickness. Liquid hydrogen is forced down the inner cylinder and returns via the space between the two cylinders. The outer cylinder will be 2-1/4" in diameter and have a wall thickness of .007". The cross sectional area between the two cylinders is relatively large, enabling us to fill with a minimum of pressure. The vacuum jacket is presently a 3-1/2" diameter aluminum cylinder having walls .028" thick. Investigation of alternative vacuum jacket materials is continuing. The present design allows target cells having different diameters but the same overall length to be interchanged. The concentric tubular design presents a uniform azimuthal distribution of mass to particles leaving the target. The liquid hydrogen and container walls range out protons of less than 225 MeV/c momentum emitted at 90°.

C-2. The LASS Vertex Detector

The LASS vertex detector consists of an assembly of cylindrical proportional and spark chambers surrounding the hydrogen target. It has

been designed to measure in the simplest geometrical fashion, the particles emerging from the target at large angles with respect to the beam direction. At the same time, by virtue of its small mass in the forward direction, it causes only a minimal amount of multiple scattering for particles at small angles to the beam direction. This is obtained by using a very light construction, consisting, apart from the chamber wires, of only mylar, styrofoam and glue in the forward and sideways directions from the target. There is significant mass only outside the chambers and on their upstream end. The detector consists of six chambers with increasing radii, ranging from 2 to 22.8". Of these, the smallest is CP_1, a 160 wire propotional chamber and the rest are spark chambers CS_1-CS_5 containing a total of 10,272 wires. Their radii are 2.0", 4.4", 6.4" 8.4", 12.4", and 22.8" respectively. The wire spacing of the proportional chamber and all but the largest spark chamber is 2 mm. The largest spark chamber has a 4 mm wire spacing. A particle emitted from the target with a completely transverse momentum of 500 MeV/c will be measured in the 25 kG field of LASS to ± 1% (HWHM).

The four inch diameter proportional chamber surrounding the target is useful in several ways. Good spatial resolution is important near the target, where the track density is the highest. Its fast response makes it useful in many trigger schemes, and its small size and low number of wires makes possible light construction, strong enough to sustain the pressure required to stress the chamber wires. The wires used are the standard 20 micron wire, supported in the middle of their 36 inch span. The cathodes are 25 micron thick aluminum bonded to mylar and glued to the surfaces of styrofoam tubes.

The five wire spark chambers each consist of two gaps and three read-out planes, thus providing a total of fifteen planes. Each chamber is designed to determine the ϕ-coordinate with good accuracy and the

z-coordinate with less accuracy. In order to do this, the first gap of each chamber has its two sets of wires crossed at a small relative angle, 2v, given by tan(v)=1/10 to produce "small angle stereo". This gap thus measures both ϕ and z with, respectively, "good" and "bad" resolution, except for the ambiguities resulting from multiple sparks in crossed wire systems. These ambiguities are resolved by the second gap, with ground plane wires parallel to the cylinder axis. The high voltage plane in this gap is 0.5 mil aluminum bonded to the other side of the mylar which supports the high voltage wire plane of the first gap. Each wire plane is simply constructed by gluing 5 mil copper coated aluminum wire onto mylar with a 1 mil layer of Scotchcast 225. The mylar is then cut to length, rolled into a cylinder and glued together. The wires are placed with zero cumulative error, so that the angle of any given wire projected back to its upstream end, is given simply by $\phi = \frac{2\pi}{N} n$ with an accuracy corresponding to plus minus 1/4 wire spacing, where n is the wire number in the plane and N is the total number of wires in that plane. The downstream end of the chambers is a 10 mg/cm^2 thick set of concentric styrofoam rings glued between the mylar cylinders. The total thickness of each chamber is equivalent to 30 mils of mylar for particles going through at right angles. The whole structure, including the read-out electronics (see below) is supported by a similar structure of successive lucite rings in the upstream end and an outer structure consisting of lucite rings and aluminum bars.

Due to the high magnetic field, a (single wire) capacitative readout system has been used. Since it contains novel features, it will be described here. Figure 4 shows the circuit (almost identical for wires on the high voltage and ground planes), consisting of three parts: a diode-rectifying circuit that stores the spark current on a capacitor, an RC filter, and one bit of a shift register.

The current sensitive rectifying circuit charges the first (integrating) capacitor to typically -40V (its sign being independent of any ringing of the spark current). This signal is then filtered through the RC filters to produce negative signals at the input of the shift registers more than 100 μs after the spark noise has died out. Because of the long time constants, it is possible to use long (25 ft.) cables to connect the rectifying circuits, (on PC boards on the upstream end of the chamber) to the shift registers (placed in card files with easy access, away from the chambers). Each wire is connected to one bit of an 8 bit shift register. After 200 and 450 μs respectively, the shift registers on the HV and GND planes are loaded in parallel, then shifted out serially at a 4 MHz clock rate.

C-3. LASS C-D Spark Chamber Modules, CD_1-CD_7

To measure particle paths in the LASS solenoid and in the region between the solenoid and the downstream dipole, a 60,000 wire spark chamber system is being built based upon mechanical designs previously developed by Group B, but requiring new electronic design because of the high ambient magnetic field. There are seven identical spark chamber modules, four in the solenoid and three between solenoid and dipole. Each has two gaps with both the high voltage and ground side of each gap being read. The wire planes of the first gap are oriented at 90° relative to each other, giving x,y spark coordinates. The second gap wires are $\pm 30^\circ$ to the vertical, to allow separation of false from true x,y pairs in multi-track events. The sensitive region of each plane is roughly 5' x 5'.

The wire sense circuit and read out logic are new designs, drawing upon work by Pizer (CERN), Jensen and Pine (Caltech), Porat (SLAC) and Nunnamaker (Chicago). Each wire is attached to ground through a small

resistance, 1Ω, which shunts most of the spark current to ground, minimizing the spark voltage pulse on the wire thus reducing spark spreading to adjacent wires and protecting components.

The sense circuit is basically a diode-capacitor peak detector which detects and stores the wire voltage until a controller scans the system and locates all wires having charged capacitors.

Each controller is a small computer itself, running on its own clock independently of the experimental on-line computer, a PDP-11. There are two controllers, one scanning ground planes, the other the high voltage planes, at a scan rate of 16 wires/μsec. If a spark is found the controller formats spark location and width and transfers this information to the PDP-11 through direct memory access in 10-20 μsec. It requires 2 msec to to scan all seven modules plus another 2 msec for data transfer for the expected seven tracks average through the system.

For single tracks in the chamber, read out efficiency is 95+% and space resolution is one half the wire spacing of 28/inch. The average spark width is 1.2 wires.

Read Out efficiency, spark widths, and resolution have not yet been measured for multiple track events.

C-4. Proportional Chamber Description

A variety of Proportional Wire chambers have been designed for the LASS spectrometer. Beam chambers, Plug chambers, and "1.5" ("2.5") chambers are being built here at SLAC while the Hodoscope Chambers are being constructed at Johns Hopkins and the cylindrical chamber at Cal Tech. A brief description of each follows, together with the read out electronics, which is the same for all proportional chambers.

(a) Proportional Plug Chambers, P_1 - P_4. These chambers are similar to the

beam chambers in design in that they too are 1 mm wire spacing chambers. Each readout plane has 256 wires. There are 3 planes per chamber giving us x,y, and e information. The sense wires are approximately 2 meters long--stretching across the bore of the solenoid, but they are desensitized in the region exterior to the central (256 mm x 256 mm) area. This allows us to keep the support frames out of the region of interest--but requires us to support these wires (in the deadened region) with mylar strips.

(b) PWC1.5 - Full Bore Proportional Wire Chamber.

Chamber "1.5" is a 2 mm proportional chamber having 4 readout planes (x,y,~~e~~, and p). Each plane has 750 wires and covers an area roughly $1\frac{1}{2}$ meters in diameter. The two primary purposes of this chamber are to provide a means of obtaining in time position information to aid background elimination in the geometric reconstruction program, and to provide a position detector which would be useful as part of a fast trigger system. This chamber is to be placed between Chambers 1 and 2 (hence its name) and is roughly 1 meter downstream of the target center. Chamber "2.5" and "3.5" when built will have the same design and serve the same function.

(c) PWH - Proportional Chamber Hodoscope

The desire for in-time position information in the forward spectrometer to aid track finding prompted the decision to construct proportional wire chamber hodoscopes on either side of downstream magnet. Each chamber has a single plane of 512 vertical wires spaced 4 mm apart, providing horizontal position information. The chamber sensitive area is approximately 2 meters across by 1 meter high.

(d) Read Out Electronics

The read out electronics is placed remotely from the PWC wires. Each PWC wire drives a 95Ω coaxial cable, which is terminated in 95Ω, connecting it to the read out electronics. This low resistance loading of each wire decreases the output pulse width ($t_R \sim t_f \sim 20$ nsec) increasing

the time resolution of the chamber at a sacrifice in pulse height, which is compensated by increased amplifier gain. The effective discrimination level is 200 μV, so typical signals of 3 mV amplitude are detected with essentially 100% efficiency. After amplification, discrimination and conversion to a standard TTL pulse, the signal is stored in a RAM used as a shift register memory, clocked at 40 MHz. With the delayed arrival of an event signal, the clock is stopped and the appropriate shift register positions scanned. This type of data storage is deadtime-less, so there is no decrease in the chamber time resolution due to the electronics, and the time delay and bin width can be varied under computer control. Fast TTL signals from each wire are available for trigger decision logic and fast analog signals are available from each plane for a multiplicity trigger.

C-5. Magneto-Strictive Read Out Chambers

Following the dipole are four plane wire spark chambers MS_1-MS_5, mechanically the predecessors of CD_1-CD_7, but using magneto-strictive wire for spark read out. Their space resolution is ± 0.3 mm. MS_1, MS_2, and MS_5 have 5' x 10' sensitive area, MS_3 and MS_4 (the super chambers) are new 6.5 x 13 ft. chambers. As with the CD chambers there are 4 planes with wires at 0 and 90° to the vertical, and + and -30° to the vertical.

The conventional M-S read out system of assigning several scalers to each M-S wire, with the associated problem of the many extra scalers required to handle peak loads, is not used here. The data recording for these chambers is done by having each delayed spark signal from the M-S wire transfer a master clock reading into shift register memory, together with the identification address of the wire giving the signal. This method is described in SLAC-PUB-994.

C-6. Scintillation Counter Hodoscope

The two hodoscopes HA and HB, are formed of scintillation counters, set edge to edge. Each hodoscope is composed of two picket fence arrays divided at the beam line, as shown in Fig. 5. Each scintillation counter is event gated and its output is stored in an array of registers.

C-7. $\check{C}_1$ - 37 Element Threshold Čerenkov Hodoscope

This is an atmospheric pressure threshold Cerenkov counter currently being designed, which is situated at the end of the solenoid (see Fig. 1). This counter will provide mass identification for particles exiting the solenoid magnet, and complement the information from the pressurized Cerenkov counter situated behind the downstream magnet.

The counter consists of 37 separate optical elements, each with its own phototube and read-out system. Three sizes of cell are used--20 x 20 cm around the beam hole where the particle density is highest, 30 x 30 cm for intermediate radius and 40 x 40 cm at the outer periphery of the solenoid.

The light collection system for each cell is shown in Fig. 6. Aluminized mylar reflector coats the sides of the radiator section and of the long light collection tube used to keep the phototube array from the solenoid's fringe field. A 45° stretched Al foil mirror reflects the Cerenkov light down this collection tube. A Fresnel lens, machined out of UVT plastic, is then used to image all of the light from the mirror on the 50 mm photo-cathode of a 56 UVP photomultiplier. The cell sizes were chosen to (a) minimize the number of "accidentals" in which two particles from the same event pass through the same cell, and (b) provide enough path length in the radiator so that particles emerging from the solenoid at the maximum possible angle give enough Čerenkov light in the

cell to make an efficient counter. Monte Carlo studies indicate that the "accidentals" level for the configuration described above are at most 3%, and that the average number of photo-electrons expected varies from a worst case (large angle particle in the short cell) of ~ 4-5 photo electrons to a best case (straight through the longest cell) of ~ 22 photo-electrons.

The threshold characteristics of this counter will be changed by using different gases as the Čerenkov radiator. A table showing the threshold momentum for π, K and protons for a selection of gases at atmospheric pressure is attached. (Table 3).

This counter will prove good π identification over a useful range of momentum and will be able to handle high multiplicity events.

C-8. $\check{C}_2$ - Large Aperture Čerenkov Hodoscope

This is a large, wide-aperture Cerenkov detector situated at the downstream end of LASS (see Fig. 1), which may be used as a hodoscope of eight optically-independent Čerenkov cells or as a simple uniformly efficient counter. The optical system is designed such that each of the eight mirrors reflects the Čerenkov light into a corresponding light horn and phototube (see Fig. 7). Notice that the different optical units are not physically separated, but if the Cerenkov cone of a particle intersects only one mirror, it will be detected only by the opposing phototube. The radiator is normally Freon 12, chosen for its relatively high index of refraction and good transmission of ultra-violet light. The individual pulse heights of each of the eight photo tubes are recorded thus providing off-line the total pulse height from the counter for each event.

The main frame of the counter is a rectangular, steel box designed to operate at pressures between 0 and 3 atmospheres. The entrance window (2mm thick Al) is 2.5 x 1 meter and the minimum path length in the radiator is 1.75 meters. At the back of the counter there is a plane of mirrors covering a total area of 2.5 x 1.25 meters and consisting of eight square sections of spherical mirrors (radius of curvature of 1.75 meters), set edge to edge. Each of the upper four mirrors is inclined at an angle of 10° with respect to the vertical in that it reflects light into one of the upper four light horns; similarly, each of the lower mirrors was inclined to reflect light into one of the lower light horns. The horns are designed to accept all light rays which have an angle with respect to the axis of the horn that is less than a maximum cut-off angle of 25°. The light from each horn is detected by a single photomultiplier tube (Amperex 58 UVP) having a photo cathode diameter of 110 mm. The optical system was designed to detect Čerenkov radiation in the ultra violet region (down to 2300 A°), so care was taken with the mirror and light horn reflectors and quartz ports and quartz-window phototubes were used.

The uniformity of light collection is good. Fig. 8 shows the light from a particle passing through the crack between two mirrors compared to the light collected when the particle was focussed on the center of a mirror. The two pulse height spectra are very similar, and may be fit with a Poisson distribution characteristic of $\sim$ 13 photo electrons. (The counter was filled with Freon 12 at 1.25 atmospheres) The counter efficiency has been measured to be 99.9%.

For further details on this counter, see H.H. Williams et al., SLAC-PUB-1070, H.H. Williams (thesis) SLAC-Report-142.

D. Trigger Instrumentation

Due to the combined effects of the large acceptance of the LASS solenoid and the long LH target, triggering the LASS spark chambers on all target interactions will produce an overwhelming amount of data. To restrict the number of events, various approaches to triggering LASS are being studied.

The E-75 spectrometer, used by Group B prior to LASS, was triggered on multiplicity, as measured by scintillation counter hodoscopes downstream of the dipole, such as HA and HB. Extension of this technique directly to LASS will probably not be satisfactory for most experiments because here a smaller fraction of the secondaries reach the dipole. However, multiplicity counting in the solenoid may be done using the fast read out of the proportional wire chamber surrounding the target, CP1 and P1.

Even more sophisticated triggers may be developed employing the fast read out of proportional wire chambers, either by combining sense wire outputs or using the induced signal on the high voltage planes. An example of such a system, taking advantage of the correlation between P_T and P_L in a solenoid field, is described below. Suppose one wishes to make a selection on a particular region of momentum transfer (e.g. $P_T > 1$ GeV/c). P_T is given by $P_T(\text{GeV/c}) = (3.7 \cdot 10^{-3}) \frac{\theta}{\Delta\phi} \Delta z$ (cm) ($\theta, \Delta\phi$ in same units). θ is the production angle, $\Delta\phi$ is the azimuthal variation of the secondary (as measured from the center line of the solenoid, not from the center of curvature) in an interval Δz along the center line. For detectors placed at fixed Δz, a minimum allowed P_T means a maximum allowed $\Delta\phi$. To serve as general trigger source detectors, three additional PWC are being placed in the solenoid, in

the gaps between CD1-PWC1.5, PWC1.5-CD2 and CD3-CD4 (Fig. 9). Each of these would be divided into 240 $1.5^{o}\phi$ segments and several radial segments to measure θ. To trigger on large P_T, a coincidence would be made between any ϕ element in the first detector and the same or neighboring ϕ element in one of the downstream detectors, indicating $\Delta\phi$ less than of the order of $2\text{-}3^{o}$. For elements at larger radius (larger θ) more of the neighboring elements would be included in the coincidence.

Preliminary studies indicate that this trigger would be satisfied by about 10% of the total cross section, with half the triggered events having P_T greater than 1 GeV/c.

These PWC elements and the scintillator hodoscopes will provide a flexible trigger system for LASS, allowing selection of sideways multiplicity, forward multiplicity, P_T and P_L.

E. LASS Data Acquisition System.

The magnitude of the data from a single LASS event, combined with the high trigger rates expected, create data flow rates too high to be handled by previous data acquisition systems used at SLAC. A new data acquisition system is being put together using state-of-the-art data transmission devices. This system makes use of a high-speed data link to the SLAC Triplex S370/360 and the new high density (6250 BPI) tape drives. In addition to providing high density data recording, this link makes available to the experimenter powerful online programming possibilities.

The overall computer arrangement is shown in Fig.10. The data is collected by controllers associated with the different types of detectors located either in the control room or in the experimental building. These controllers pass the data from the individual detectors to the DEC PDP11/20 minicomputer which assembled and compacts the data into an event buffer for transmission via an IBM System 7 over a coax link to the S370/360. Event data is also sent to an IBM 1800 at a much slower

sampling rate for local monitoring and display. An experiment control panel is used by the experimenter to determine the flow of data to the various computers.

The PDP11/20 serves as the central "traffic cop" of the computer network and as a "front end" buffer for the experimental data. It is controlled from the experimenter's control panel and in turn controls the data flow to the System 7 and IBM 1800. It does no analysis or monitoring but simply keeps track of the experimental status and shuttles event buffers at high speed to the peripheral computers.

The System 7 is the local data port for the S370/360. It can buffer and transmit data to the S370/360 at rates approaching two million bits per second. It can also receive data at much lower rates from the S370/360 to pass on to the PDP-11 or IBM 1800. These transmissions will be limited to text messages and command replies to the experimenter.

The software in the S370/360 which receive data from the experiment will leave a great deal of flexibility to the experimenter. He may set up a system which merely spools data on the high density tape drives or he may define a more complicated network which allows him to interact with a complicated analysis task via the IBM 2250 graphics terminal or the Tektronics graphics display.

The IBM 1800 has beem the mainstay of spectrometer data acquisition systems in the past at SLAC. Its inclusion in LASS provides an alternative when the S370/360 is not available or when use of the S370/360 is limited by other considerations. Its peripherals include a disk, line printer, keyboard, two 800 BPI tape drives, and two graphics displays. In addition much software is available from previous experiments for monitoring of the various detectors in LASS.

The LASS data acquisition system is capable of handling the high rates possible from the physics experiment and provides some versatility in the analysis and monitoring of the apparatus.

F. LASS Software

The software for LASS, in the areas of the solenoid and real time data acquisition, has been developed in some detail over a period of about two years. The effort for the solenoid has been borne entirely by our group while the real time effort has been shared with SCIP (Stanford Computer Information Processing). The combined effort represents about five man years of work.

In order to obtain more or less realistic data, a simulator was developed which generates physics events of diverse types and then integrates the particle orbits through the magnetic fields of the system. The effects of multiple scattering, measurement resolution and energy loss are included. Additionally, one may simulate chamber inefficiencies to study their effects. The result is a set of detection co-ordinates in the wire spark chambers and other detecting apparatus.

From these simulated detections, the basic track finding algorithms and physics reconstruction have been explored for several different final states both with and without a simulated background of multipronged events. For tracks detected entirely in the solenoidal wire planes the algorithm exploited (so-called Luste algorithm) is the constant bending about the orbit axis as particle traverse equally spaced or modularly spaced measuring stations. For equally spaced chambers this translates into equal chord lengths between measurements when the orbit is projected into a plane perpendicular to the magnetic field. Since one cannot assume 100% efficient chambers, the algorithm has been extended to include the case where the chamber spacings are in simple submultiples 1:2 and 1:3. For equal spacing the algorithm requires no square roots or other costly subroutine calls on a computer and as a result proceeds very rapidly. After likely candidates are found using this algorthm, they are tested with greater rigor for consistency in the x-y, e-p substations which comprise each plane.

For tracks which are detected primarily in the cylindrical spark chambers surrounding the liquid hydrogen target, one uses a method in which there is a maximum bending angle defined for an orbit as it passes from one cylinder to the next. For credibility, four sparks are required to define a track; hence the orbit with the smallest allowable radius is the one which bends through 180 deg at cylinder four (a physics limitation of $p_T \gtrsim 75$ Mev/c for non-forward tracks). The method then proceeds to find candidates by starting from a spark in cylinder n at an azimuthal angle φ_n and scanning cylinder n+1 for sparks in the azimuthal interval

$$\varphi_n - \Delta\varphi_n^{max} < \varphi_{n+1} < \varphi_n + \Delta\varphi_n^{max}.$$

When candidates with sufficient credibility are found, they are then subjected to a simple monotony test in the z co-ordinates of the sparks and finally to a more stringent three point circle fit before they are accepted.

Reconstruction is done by performing a least squares fit of the measured points to a simple helix (the design characteristics of the solenoid are sufficiently stringent that no more complicated form should be required, though a more complex orbit could be accommodated if necessary with minor recoding). Two modes are available for this: single track reconstruction and global (entire vertex) reconstruction.

In the case of global reconstruction, all tracks in a vertex cluster are constrained to emanate from the same point. As an optional feature, kinematical constraining to a final state hypothesis may be invoked as a part of the global fit. The final result thus contains a best estimate of the vertex position.

The method of fitting is similar in both cases: a chi-squared quantity is formed from the residuals of the orbit intersections with

the various measuring stations and the measured points. The weighting of the residuals derives from a variance matrix which combines multiple scattering and wire spacing at the orbital intersections with each measuring station. Chi-squared is then linearized in the parameters of the helicies and minimized by successive interations.

In the single track reconstruction mode, one needs to make an estimate of the vertex position after fitting since this information is not a part of the fit. Proportional chambers in front of the liquid hydrogen target define the incident beam particle (and hence the interaction point) to be within a cylinder the length of the target whose axis is parallel to the axis of the solenoid and whose radius is a fold of the chamber resolution, multiple scattering in the target, and the divergence of the beam. The fitted orbit is extended to find its intersections with this cylinder. These give the upstream and downstream limits on the z co-ordinate of the interaction while the midpoint of the orbit between these intersections is taken as the vertex.

Our former spectrometers have given us much experience in handling the downstream part of the system, and substantially less developmental work has been expended in this area. We intend in the near future to incorporate most of the techniques employed in the old MIDAS into a modular new version logically separate from the solenoidal package.

The logical joining of the solenoid system and dipole system is accomplished by an impulse approximation extension of the orbits through the fringe field of the solenoid. The philosophy of this procedure is to associate tracks in the two parts of the system by a rapid and approximate technique, thus avoiding a time-consuming exact integration of the orbit through the fringe field. The solenoid measurements are used to determine the production angles of <u>all</u> the tracks and the momentum of

particles below ~ 2 GeV/c. The dipole part of the system supplies the momentum measurements of particles above 2 GeV/c, and these measurements are incorporated as independent momentum determinations in the fitting procedures described above - i.e., as separate terms in chi squared weighted by the squares of their estimated errors.

The "impulse approximation" extention of orbits through the fringe field has been tested in fair detail with simulated data. The extrapolated position deviated less than $\pm$ 0.5 cm from the true position for tracks above 2 GeV/c (and less than $\pm$ 0.2 cm for tracks above 10 GeV/c). In a sample of A_2 meson events simulated at 16 GeV/c, the median minimum separation between orbits at the last solenoidal plane was 20 - 25 cm; hence $\pm$ 0.5 cm accuracy appears quite adequate for track association.

Proportional devices in the system differentiate tracks associated with the trigger from background in virtually all cases. Large angle tracks nearly always (except at the extreme ends of the target) pass through the innermost proportional cylinder, and small angle tracks always pass through the fully proportional chamber, PWC 1.5. To the extent that these two chambers operate at high efficiency and background events are rare within $\pm$ 100 nsec of the trigger time, one can easily select the proper cluster of tracks in the solenoid. If the efficiency of PWC 1.5 is known to be high (as determined from online monitoring or preliminary sampling of a section of the data), one can save considerable track finding time by requiring this plane to fire and effectively discarding the background.

For purposes of checking out the spectrometer and for debugging solenoid algorithms and reconstruction, a graphical display package for an IBM 2250 scope has been written which allows one to display the measurements and the tracks found in the solenoid in three orthogonal

projections (x-y, x-z, and y-z projections where the field and beam are along the z axis). Results for some four prong events with a simulated background are shown in Fig. 11 . Such graphical techniques have been extremely valuable in debugging the software and promise to be equally useful in checking out the spectrometer with real particles.

The Real Time Data Acquisition System requires co-ordination of many different components: The PDP-11/IBM1800 system, the System 7 and SBCU system and finally the 370/168 (Message Router), for spooling transmitted data to tape (Spooler), and for communication via the SBCU with the System 7. Since the System 7 code needs to be tailored to our particular configuration,the programming has been done jointly by SCIP and our group. The PDP-11/IBM1800 system has been done entirely by our group.

The Message Router allows one to attach analysis, graphics and command tasks to form a real time network in the 370/168. Each task may have a number of communications nodes and similar nodes may be defined in the PDP-11 and/or IBM1800, as well as at the 370/168 operator's console. Messages (which may be either text or experimental data) can then be routed to any of these nodes in a flexible way.

This portion of the system has been tested on the Model 91 for two networks which are shown schematically in Fig. 12. The first of these has the number of nodes and configuration which will be mounted initially for LASS, but the tasks are mostly dummy ones. The PDP-11 and IBM 1800 nodes in the system were simulated by tasks in the Model 91. Testing this network gave some insights into the problems of real time communication in a moderately complex environment and demonstrated that the Message Router system was capable and well suited to mounting such a system. The second network was of simpler form but attached an analysis task with the full compliment of track finding and fitting subroutines as well

as the 2250 display package for graphical display of the events.

Additionally the Message Router has been used to transmit messages both ways between the PDP-11 and Model 91 via the System 7. Because of the heavy computing demands on the Model 91 and its non-virtual core, the task of putting together all these pieces must be deferred until the Model 168's are available. Our present plans are to check out the entire system first with simulated data from tapes which can be read on the IBM 1800, passed to the PDP-11 and entered into the network exactly as real data will be. Of course real data will be used whenever the hardware and accelerator are ready to provide it.

The offline analysis of the data may be done either in a stand-alone fashion or, using the Message Router, in a network which would allow some physics interaction and graphics abilities. Since the analysis algorithms and fitting procedures are modular, one can explore each event by degrees depending on its interest and value. The first step in this procedure, called a 'soft-ware trigger', involves decoding coordinates from the proportional chambers and perhaps other detectors and examining them to determine the multiplicity and general topology of the event. Although the process is experiment dependent, we estimate the expenditure of only a few milliseconds of Model 168 CPU time for this examination. For events which pass this test, one can then do track finding and reconstruction in the solenoid--a process which takes an estimated 50-100 milliseconds, depending on background levels and multiplicity. Finally, for events of sufficient interest, downstream reconstruction and global fitting may be invoked. The total time for a fully reduced event is on the order of 200-250 milliseconds, but the average time would be quite substantially less, depending on the number of events dropping out at each level.

Table 1

LASS Magnets

A. Solenoid

1. Inside Diameter (clear bore) = 185 cm.

2. Length (fiducial) = 350 cm.

3. Length (overall) = 465 cm.

4. Central Field = 25 kG

5. Field Homogeneity

   A) ± 200 gauss from z = 30 cm. to z = 270 cm. (Spark Chamber No. 3) R = 0. z = 0 at the upstream end of the H_2 target.

   B) ± 700 gauss, R = 0-75 cm., z = 30-270 cm. For 75 < R < 100 cm. the field varies by +25% (near the coils) to -25% (near the gaps for the spark chambers).

6. Fringe Field = 1-3 kG 3 ft. outside the iron

7. Current = 1800A

8. Inductance = 25H

9. Helium Volume = 5000 ℓ.

10. Operating Heat load 30 ℓ/hr. He 30 ℓ/hr. N_2

B. Dipole

1. Field Region: 2m wide x 2.4m in beam direction

2. Gap = 1 m.

3. $\int Bdl$ = 30 kG -m. B_{max} = 16 kG

4. Power Required = 4 MW

5. Mirror thickness = 13 cm.

6. Mirror - poles spacing = 70 cm.

Table 2
(page 1)

Beam 20-21-22

1. Length: 456 ft.
2. Acceptance: $d\Omega = 35$ μsr
3. $P_{max} = 15.5$ GeV/c
4. Magnification = 1. Momentum dispersion is also zero at the final focus. Spot Size = 1 cm (FWHM).
5. $\frac{\Delta P}{P} = \pm 2\%$ (HWHM)
6. Target = 0.9 radiation lengths of Be (30 cm).
7. Production Angle = 1^{o}
8. rf separation available for all momenta.
9. Flux:
   Particle fluxes may be calculated using the following formula, which is accurate to ± 30%.

$$Y = C \ln \left(\frac{E_o}{p+\delta}\right) e^{-\left(\frac{Q}{Q_o}\right)^2} \quad \frac{\text{particles}}{\text{primary elec., GeV/c, sr}}$$

   E_o = primary beam energy (18 GeV)

   C, δ, Q_o are taken from the table below

   p = beam momentum in GeV/c

   Q = transverse momentum = p sin 1^{o}

	C	δ	Q_o
$\pi^{\pm}$	$16. \times 10^{-4}$	1.5 GeV/c	.425 GeV/c
K^{+}	1.7×10^{-4}	1.5	.53
K^{-}	0.7×10^{-4}	1.85	.53

C for 0.9 rad. length Be target

Sample Calculation of pion flux at LASS

$$Y = C \ln \left(\frac{E_o}{p+\delta}\right) e^{-(Q/Q_o)^2}$$

let $p = 12$ GeV/c

$\Delta p = (.04)\ (12\ \text{GeV/c}) = .48$ GeV/c

$Q = (12\ \text{GeV/c}) \sin 1^\circ = .209$ GeV/c

$C = 16 \times 10^{-4}$ particles/primary electron, GeV/c, sr.

$\delta = 1.5$ GeV/c

$Q_o = .425$ GeV/c

$$Y = (16 \times 10^{-4}) \ln \left(\frac{18}{12 + 1.5}\right) e^{-\left(\frac{.209}{.425}\right)^2} = 3.65 \times 10^{-4}$$

$$\text{Flux} = (3.65)\ (10^{-4})\ \left(2 \times 10^{11} \frac{\text{primary electrons}}{\text{pulse}}\right)\ (3.5 \times 10^{-5}\ \text{Sr}) \times$$

$$(.48\ \text{GeV/c})\ (.80(\text{decay factor})) = 1000\ \text{pions/pulse} \pm 30\%$$

10. Spot size at final focus (F4): 90% of the flux is within 0.5 in. radius of the central ray.

Threshold momenta for various gases at atmospheric pressure.
At $\lambda_{T/2}$ the transmission of 1 meter of gas is 50%.

		THRESHOLD MOMENTUM (GeV/c)			
GAS	n-1	π	K	P	$\lambda_{T/2}$
Methane (CH_4)	4.41×10^{-4}	4.7	16.6	31.6	1500 Å
Carbon Dioxide (CO_2)	4.50×10^{-4}	4.64	16.4	31.2	1950 Å
Freon 14 (CF_4)	4.61×10^{-4}	4.59	16.2	30.8	1760 Å
Nitrous Oxide (N_2O)	5.15×10^{-4}	4.34	15.3	28.8	?
Ethane (C_2H_6)	7.06×10^{-4}	3.71	13.1	24.9	2040 Å
Sulfur Hexafluoride (SF_6)	7.85×10^{-4}	3.52	12.4	23.6	1770 Å
Freon 13 ($CClF_3$)	7.99×10^{-4}	3.48	12.3	23.4	1975 Å
Freon 22 ($CHClF_2$)	8×10^{-4}	3.48	12.3	23.4	2040 Å
Propane (C_3H_8)	10.05×10^{-4}	3.1	11.0	20.8	1880 Å
Freon 13B1 ($CBrF_3$)	10.07×10^{-4}	3.1	11.0	20.8	2600 Å
Freon 12 (CCl_2F_2)	11.52×10^{-4}	2.9	10.03	19.5	2220 Å
Butane (C_4H_{10})	14.81×10^{-4}	2.56	9.05	17.2	2230 Å
Isobutane (C_4H_{10})	14.81×10^{-4}	2.56	9.05	17.2	1820 Å
Methyl Chloride (CH_3Cl)	16.7×10^{-4}	2.41	8.53	16.2	2180 Å
Neopentane (C_5H_{12})	17.1×10^{-4}	2.39	8.43	16.0	?
FC-75 ($C_8F_{16}O$)	27.4×10^{-4}	1.88	6.65	12.7	?

Table 3

Figure Captions

Fig. 1. Schematic layout of LASS.

Fig. 2. Layout in Building 121, showing the placement of the spectrometer.

Fig. 3. Schematic of Beam 20/21 as it enters the LASS area, showing the beam instrumentation.

Fig. 4. Cylindrical spark chamber read out circuit.

Fig. 5. (a) Schematic of hodoscope A--consisting of 46 scintillation counters in two arrays above and below the beam line. All counters are 8" wide and 32" long except at the central position which has two 4" wide counters which can be withdrawn ~ 2" on either side of the beam line to leave a beam hole.

(b) Schematic of hodoscope B--consiting of 76 scintillation counters in two arrays split at the beam line. All counters are 6" wide and 32" long except at the central position which has two 4" wide counters which can be withdrawn ~ 2" on either side of the beam line to leave a beam hole.

Fig. 6. Schematic of the 32 element Cerenkov counter at the end of the solenoid. (a) end on view showing the three cell sizes employed. (b) example of the light collection system.

Fig. 7. Schematic of C_2--the pressurized Cerenkov hodoscope.

Fig. 8. Pulse height spectra from C_2. (a) and (b) are from neighboring mirrors with the beam passing through the center between them. (c) is the sum of pulse heights from the two mirrors. (d) is the pulse height when the beam passes through the center of a mirror. The distributions (c) and (d) are very similar.

Fig. 9. Schematic of the elements of a PWC used as a trigger source and proposed location of such chambers in the solenoid.

Fig. 10. Schematic of the data collecting and transmitting computers.

Fig. 11. Computer driven oscilloscope displays of two events--solenoid only.

Fig. 12. Schematic of the full computer configuration, showing the networks for data collection and recording and event reconstruction and interaction with the experimenter.

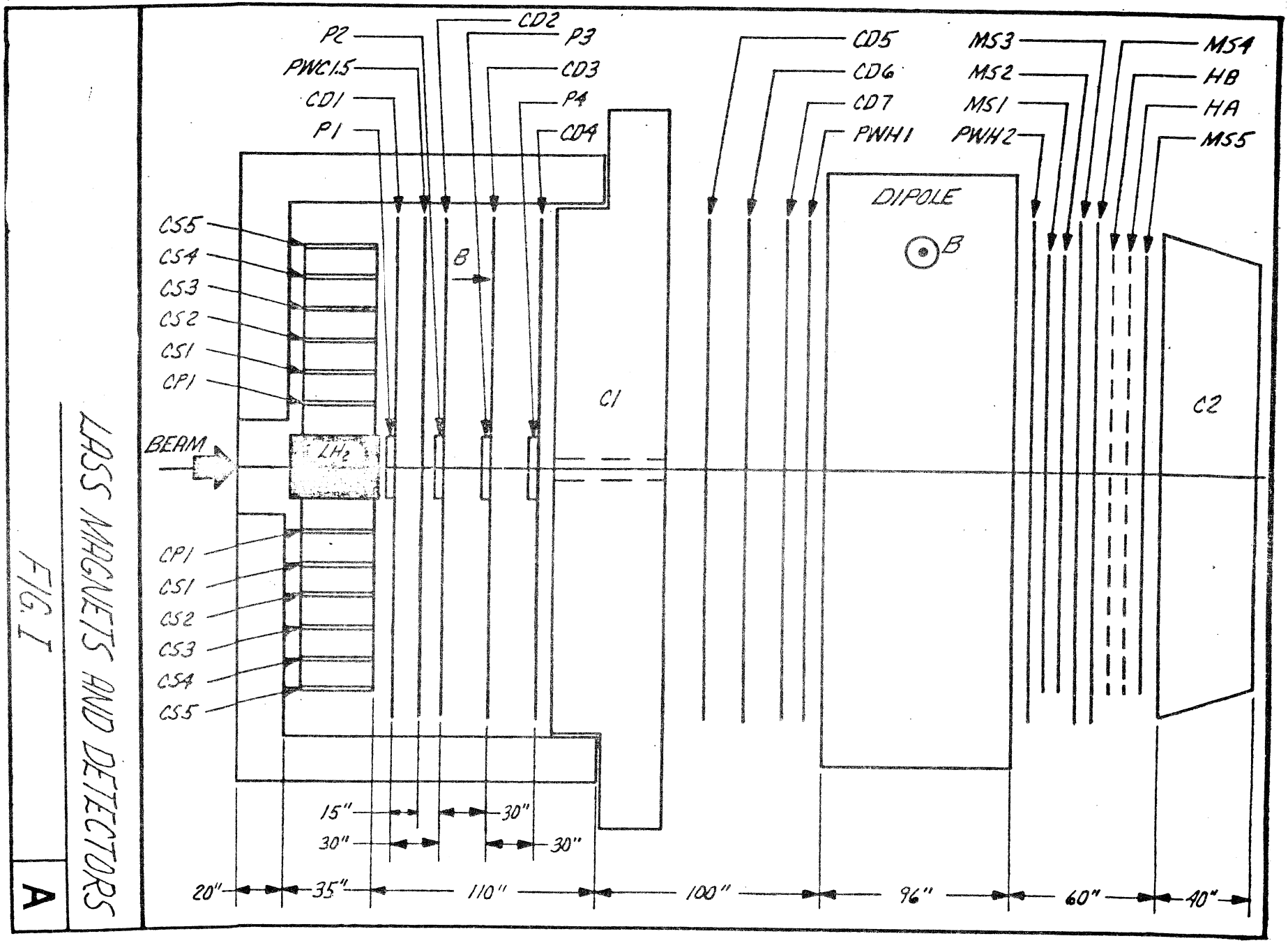
LASS MAGNETS AND DETECTORS
FIG. 1
A
P2
CD2
P3
PWC1.5
CD3
CD1
P4
P1
CD4
CD5
CD6
CD7
PWH1
MS3
MS2
MS1
PWH2
MS4
HB
HA
MS5
DIPOLE
B
CS5
CS4
CS3
CS2
CS1
CP1
BEAM
LH2
C1
C2
15"
30"
30"
30"
20"
35"
110"
100"
96"
60"
40"

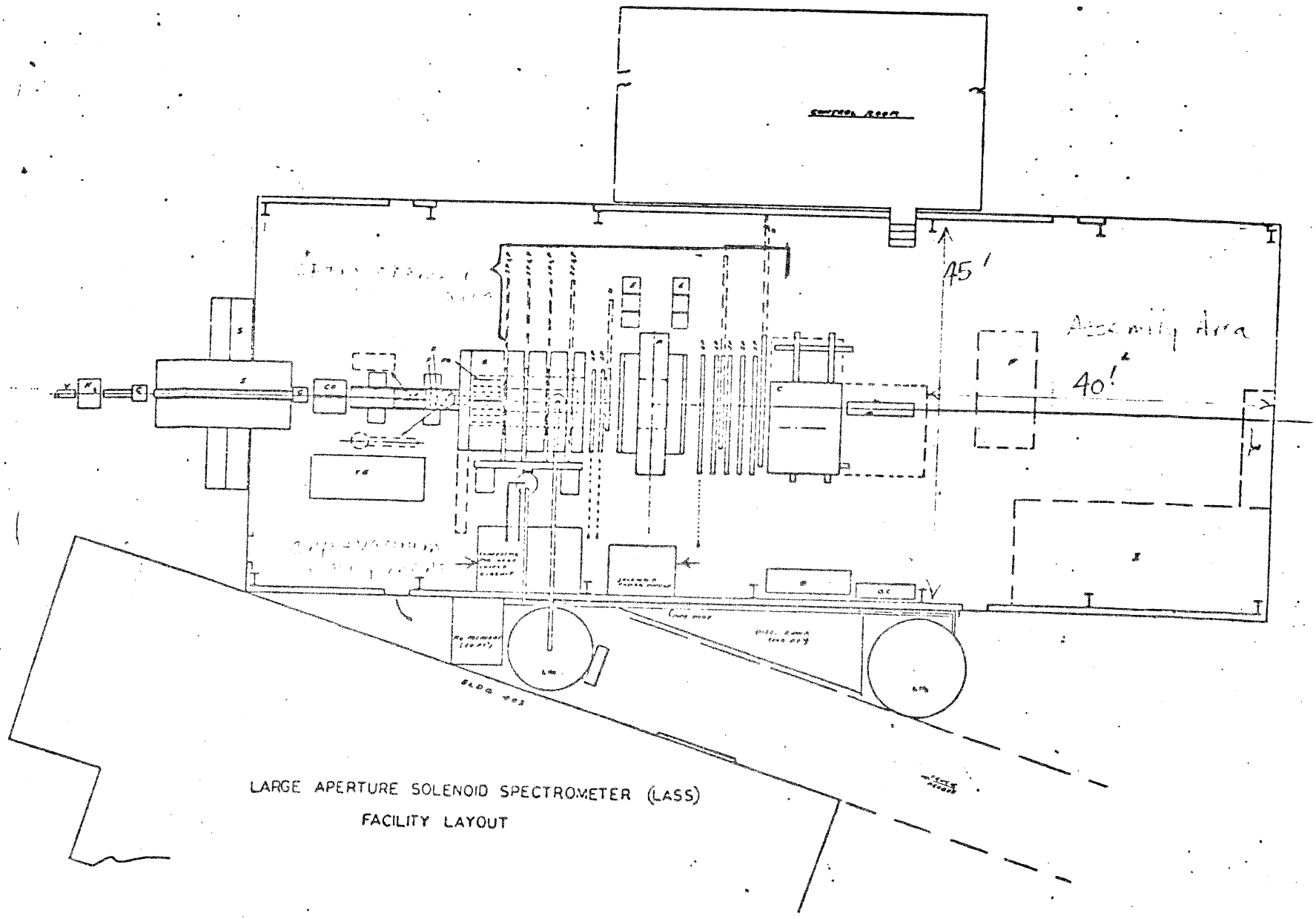

Figure 2

LASS Building

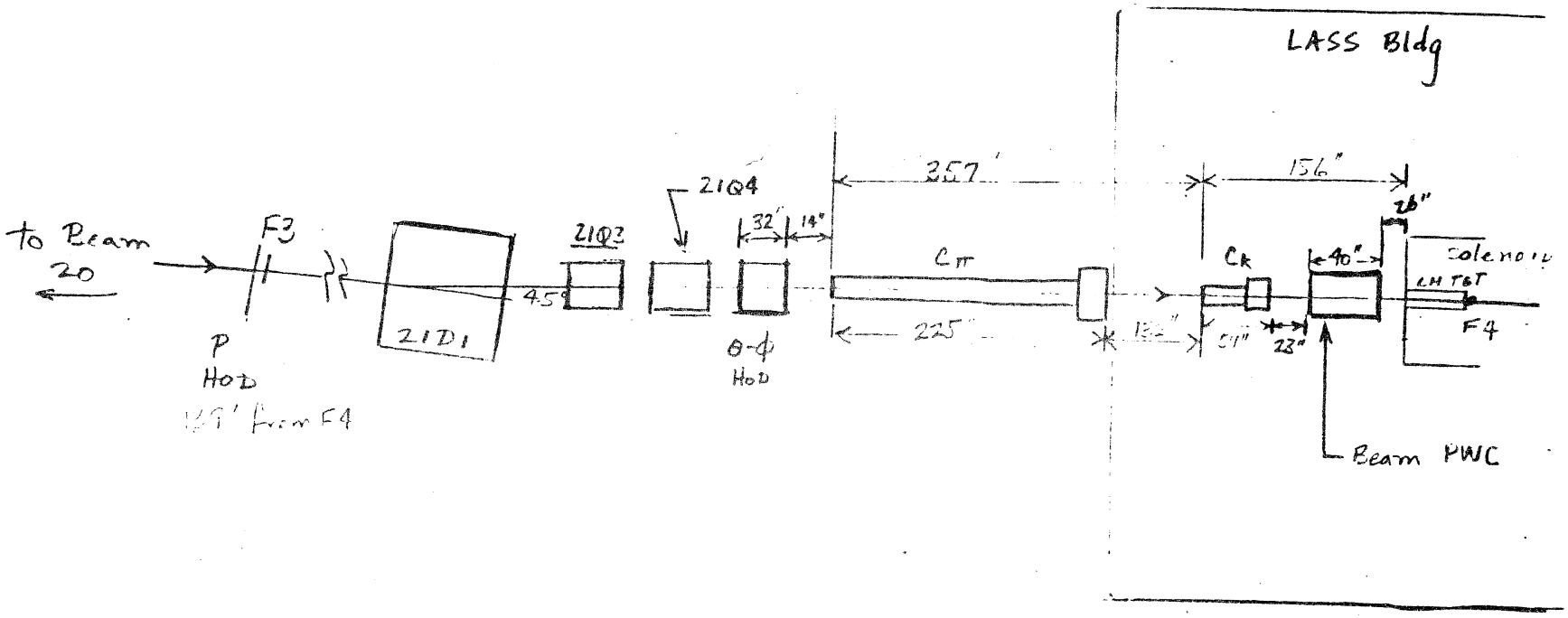

Figure 3

Beam 21 Instrumentation

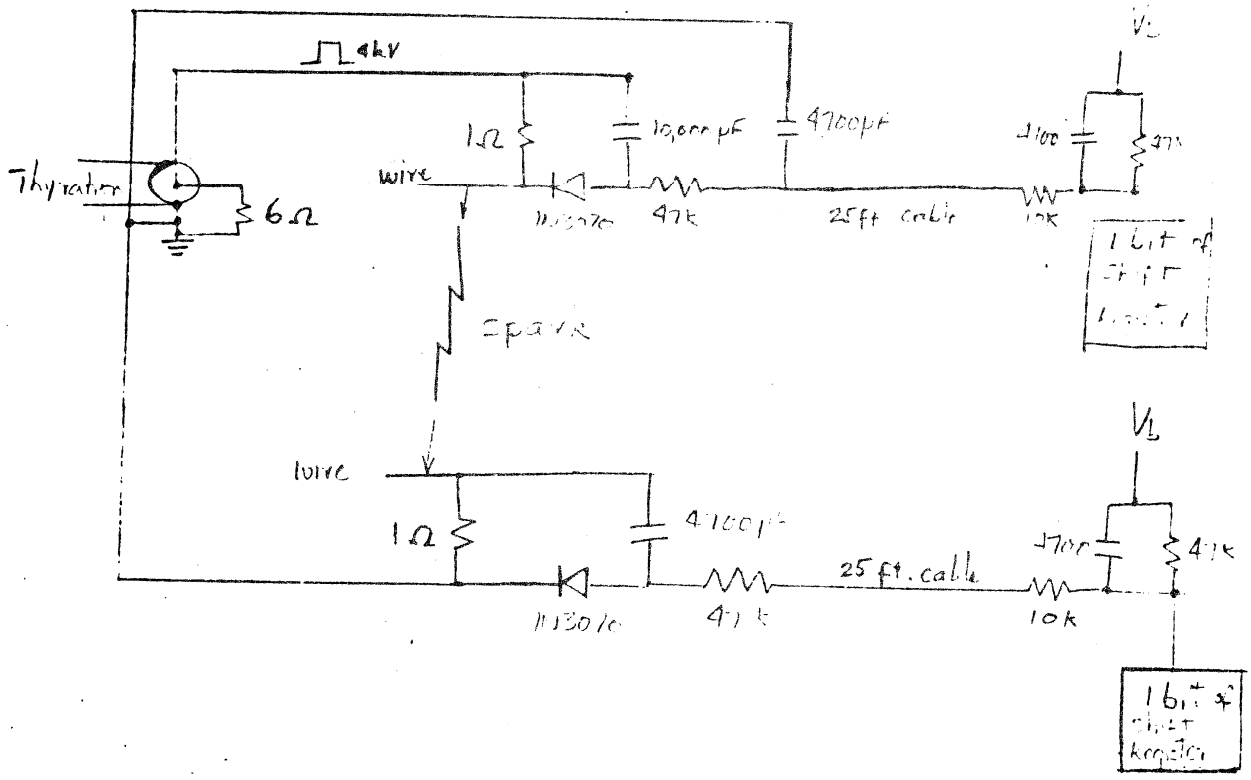

Figure 4

Cylindrical Spark Chamber Read Out Circuit

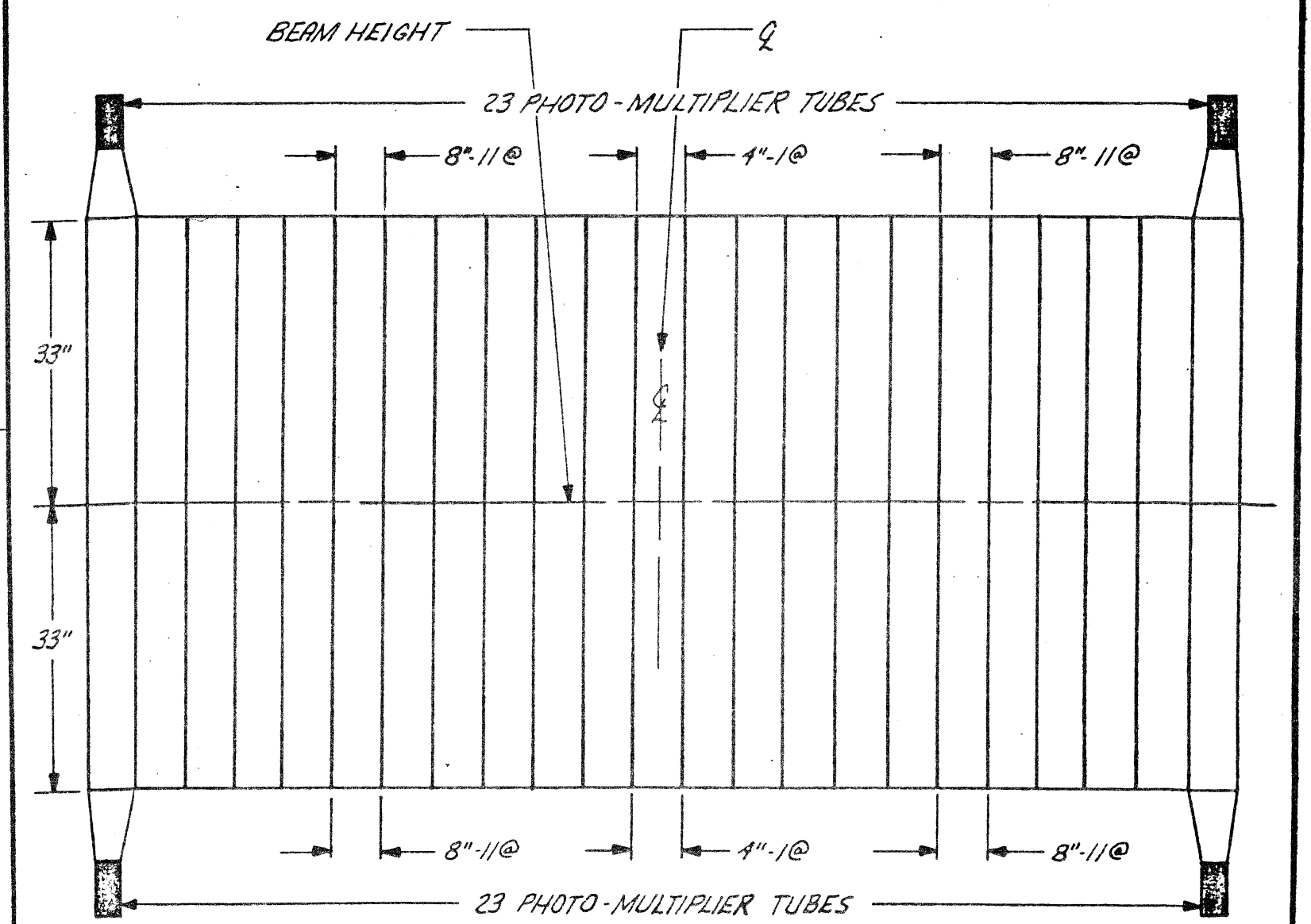

HODOSCOPE H (1H)

FIG 5a

A

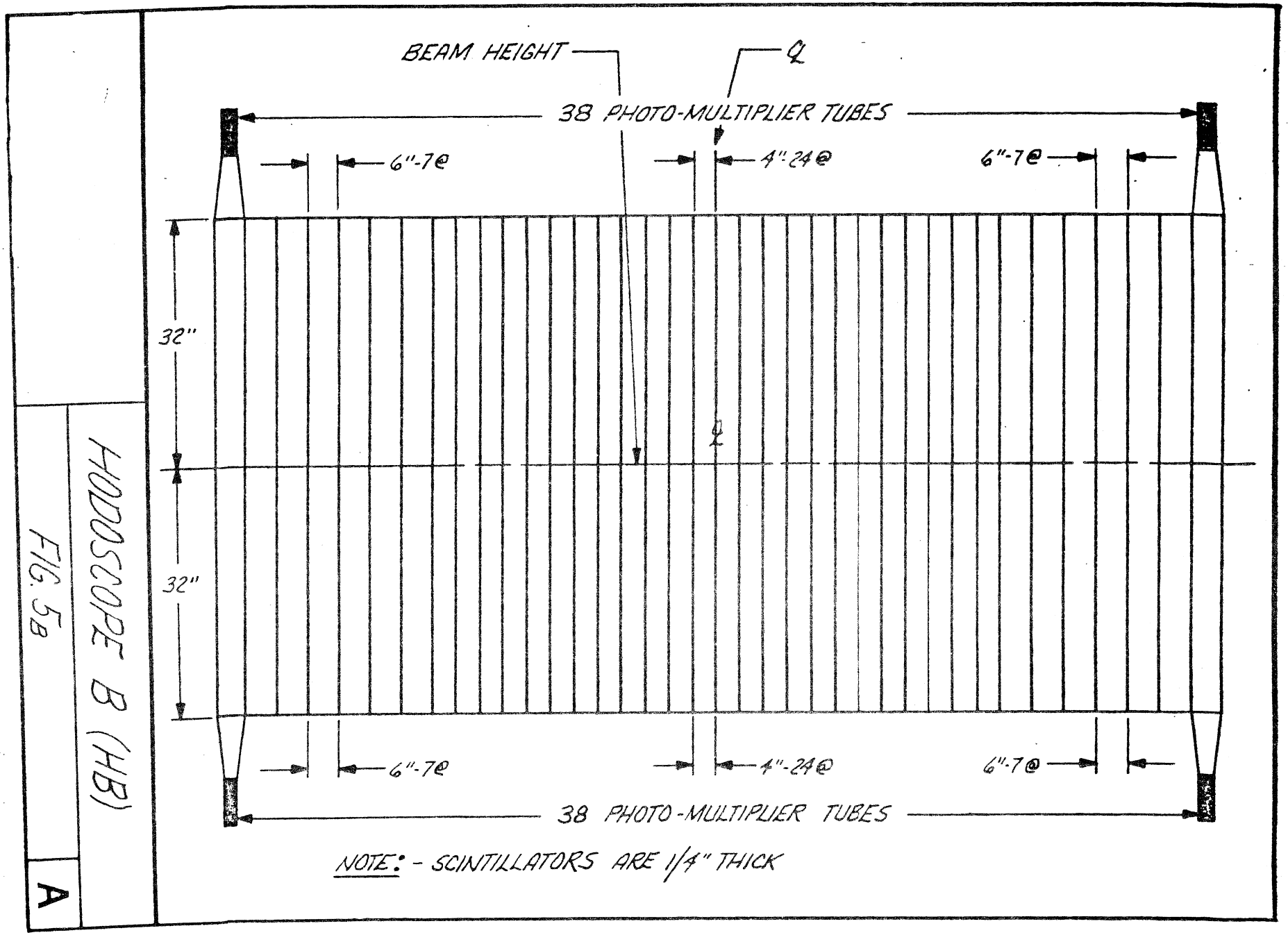
BEAM HEIGHT
℄
38 PHOTO-MULTIPLIER TUBES
6"-7@
4"-24@
6"-7@
32"
32"
℄
6"-7@
4"-24@
6"-7@
38 PHOTO-MULTIPLIER TUBES
NOTE:- SCINTILLATORS ARE 1/4" THICK
HODOSCOPE B (HB)
FIG. 5B
A

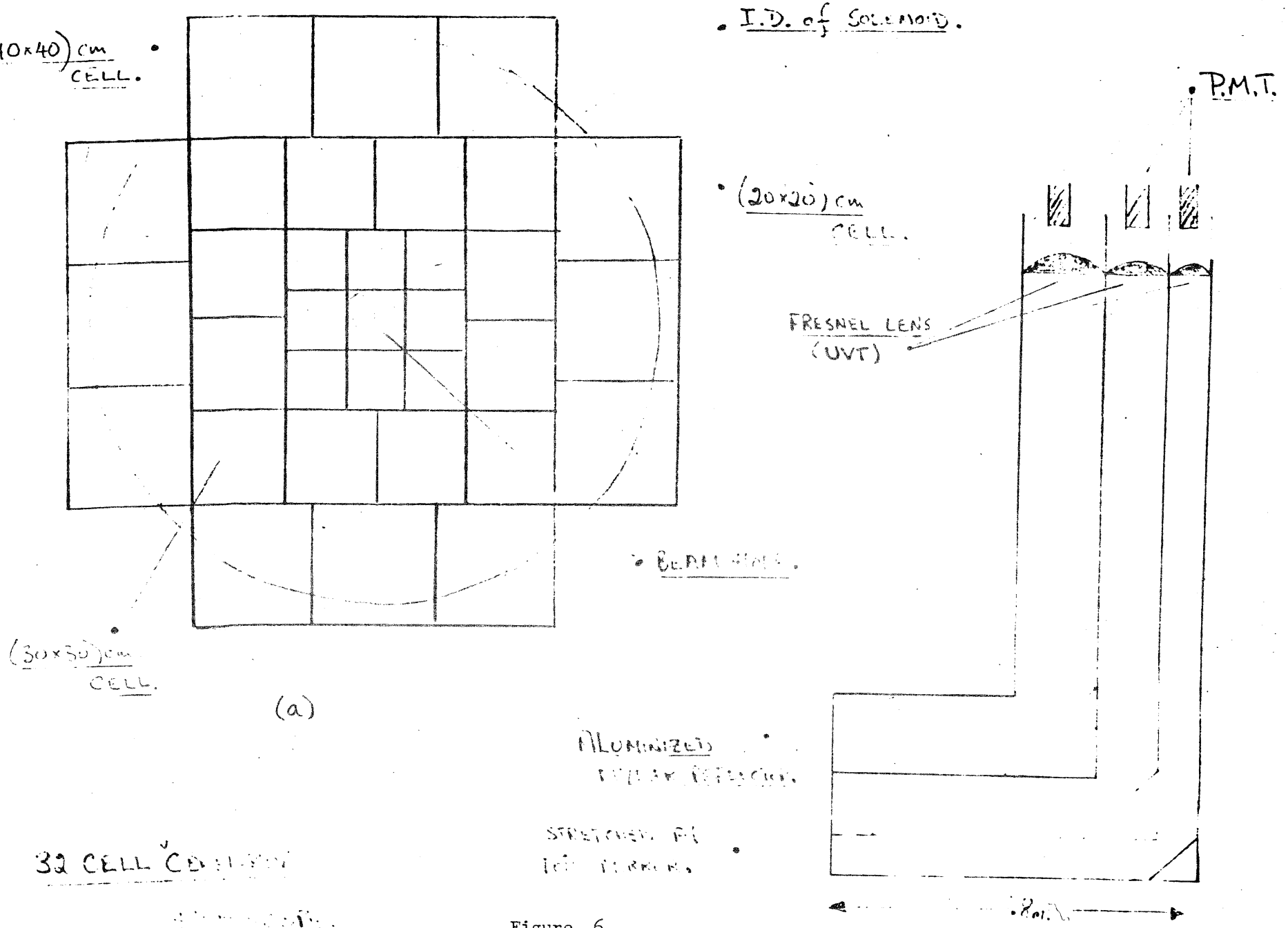
(40×40) cm CELL.
I.D. of SOLENOID.
P.M.T.
(20×20) cm CELL.
FRESNEL LENS (UVT)
(30×30) cm CELL.
(a)
ALUMINIZED
32 CELL

Figure 6

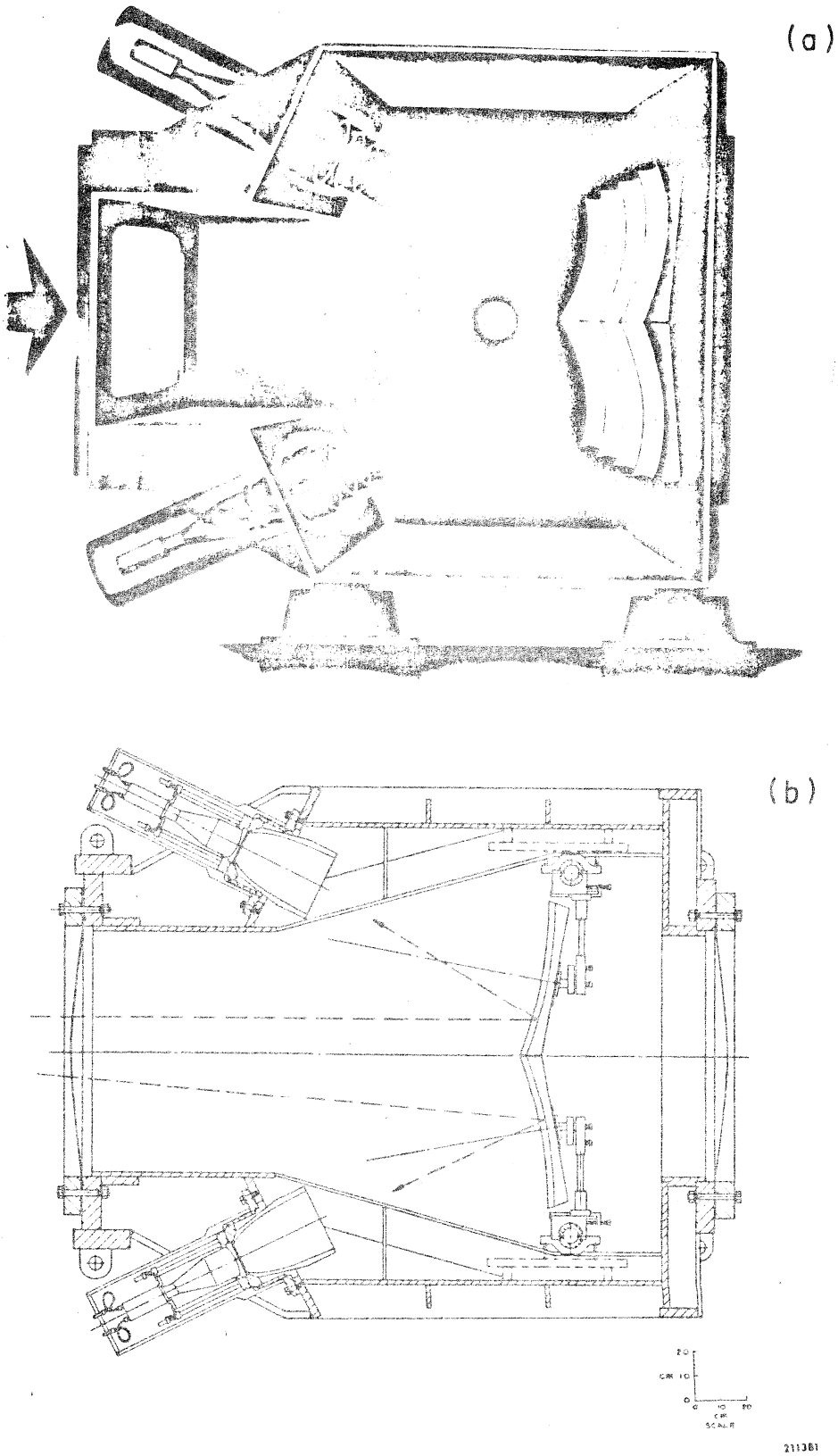

Figure 7

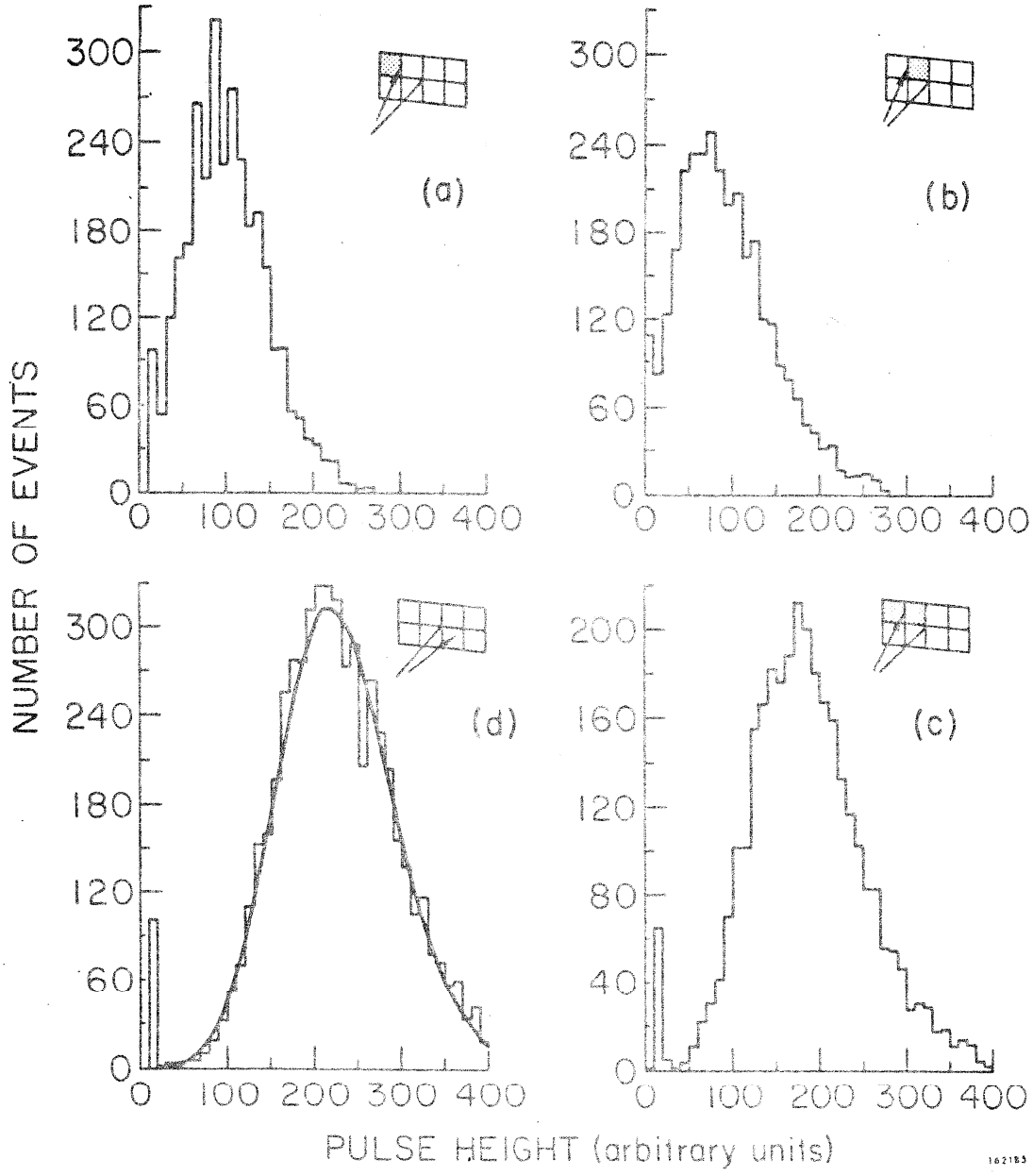

Figure 8

C2 Pulse Height Distribution

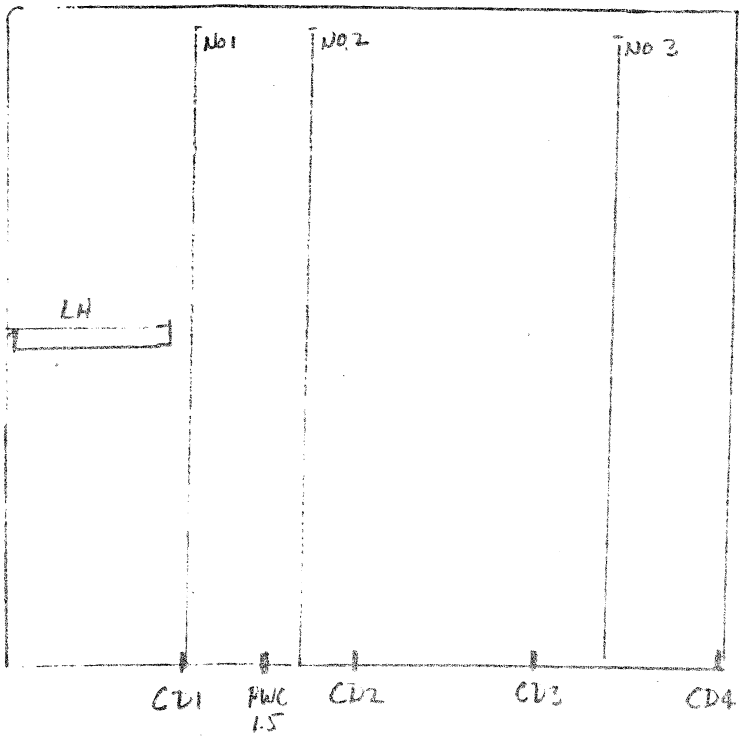

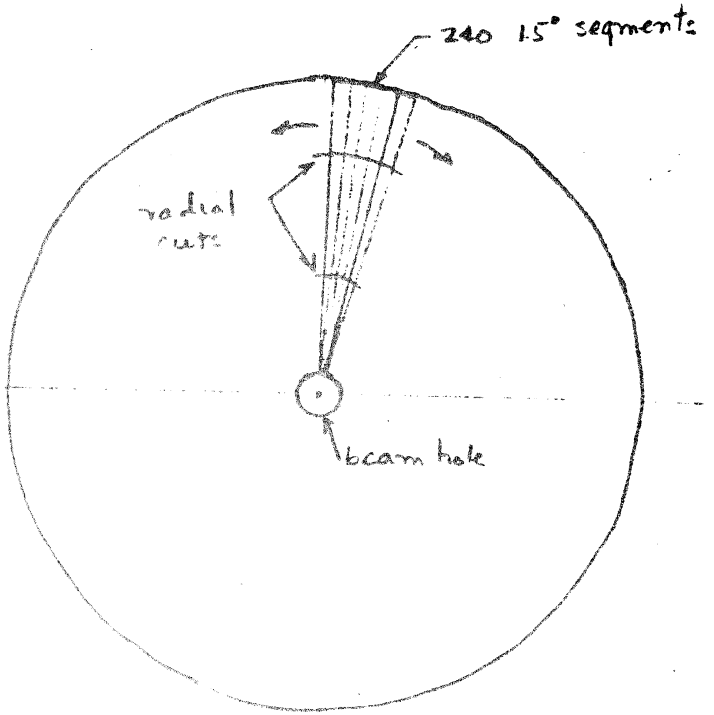

Trigger PWC	z_0	# Radial Segments
1	1.35m.	1
2	1.70	2
3	3.05	2

Figure 9

Trigger PWC

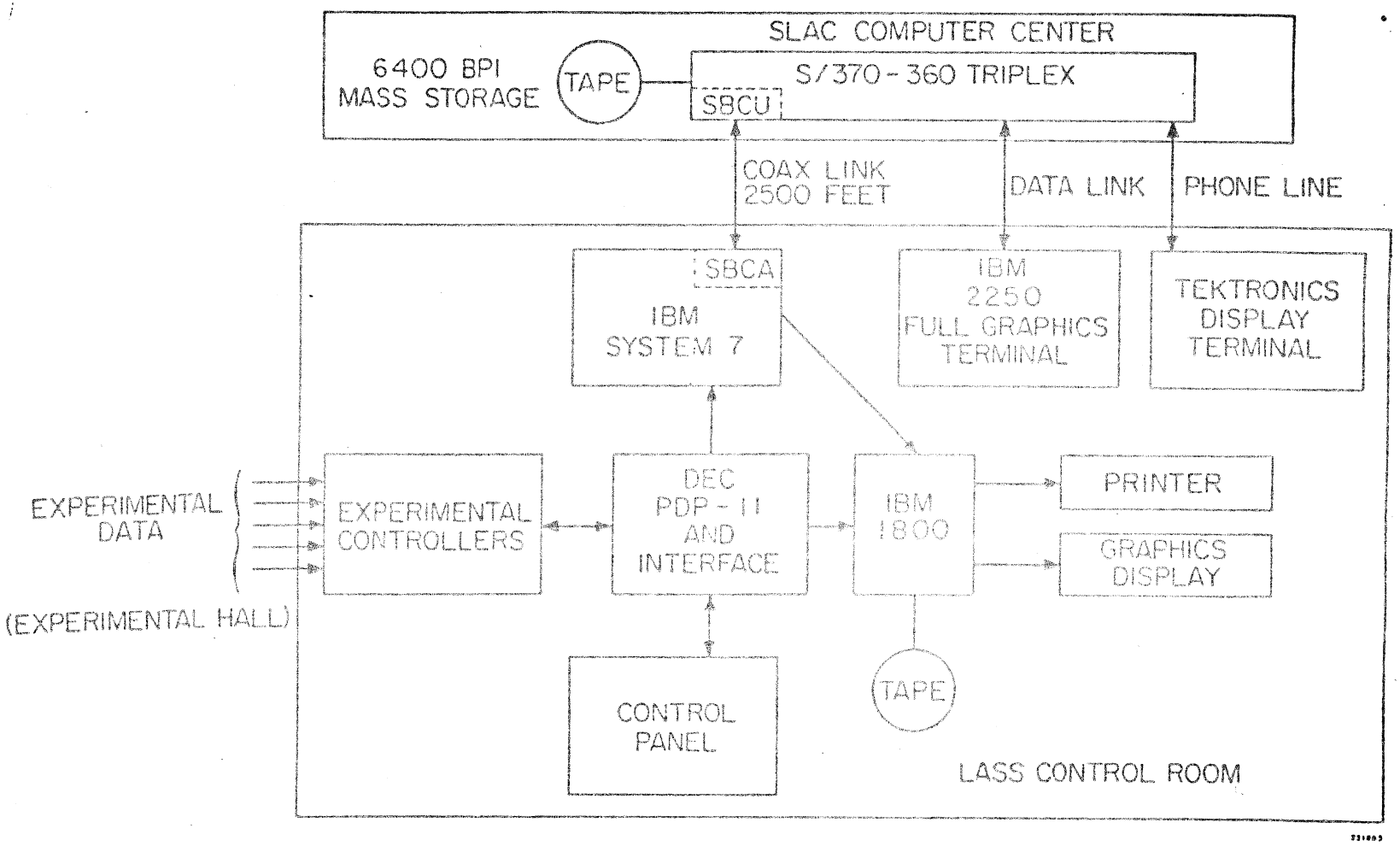

FIG. 10- Overall computer arrangement.

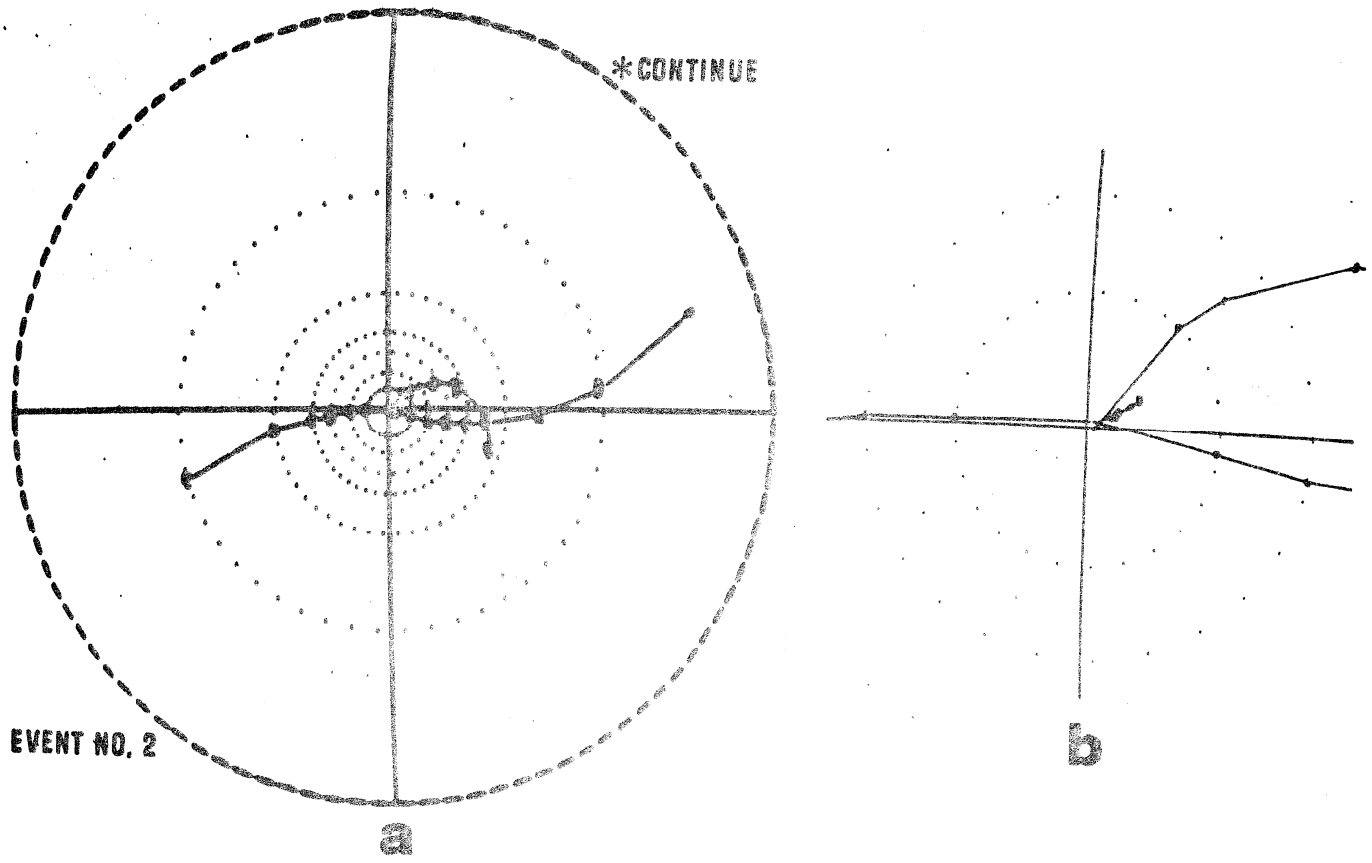

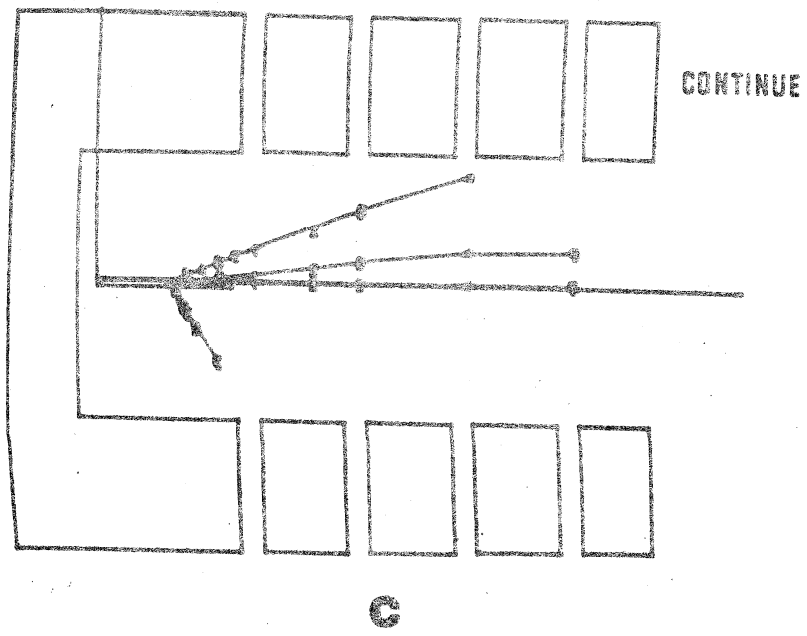

Figure 11a

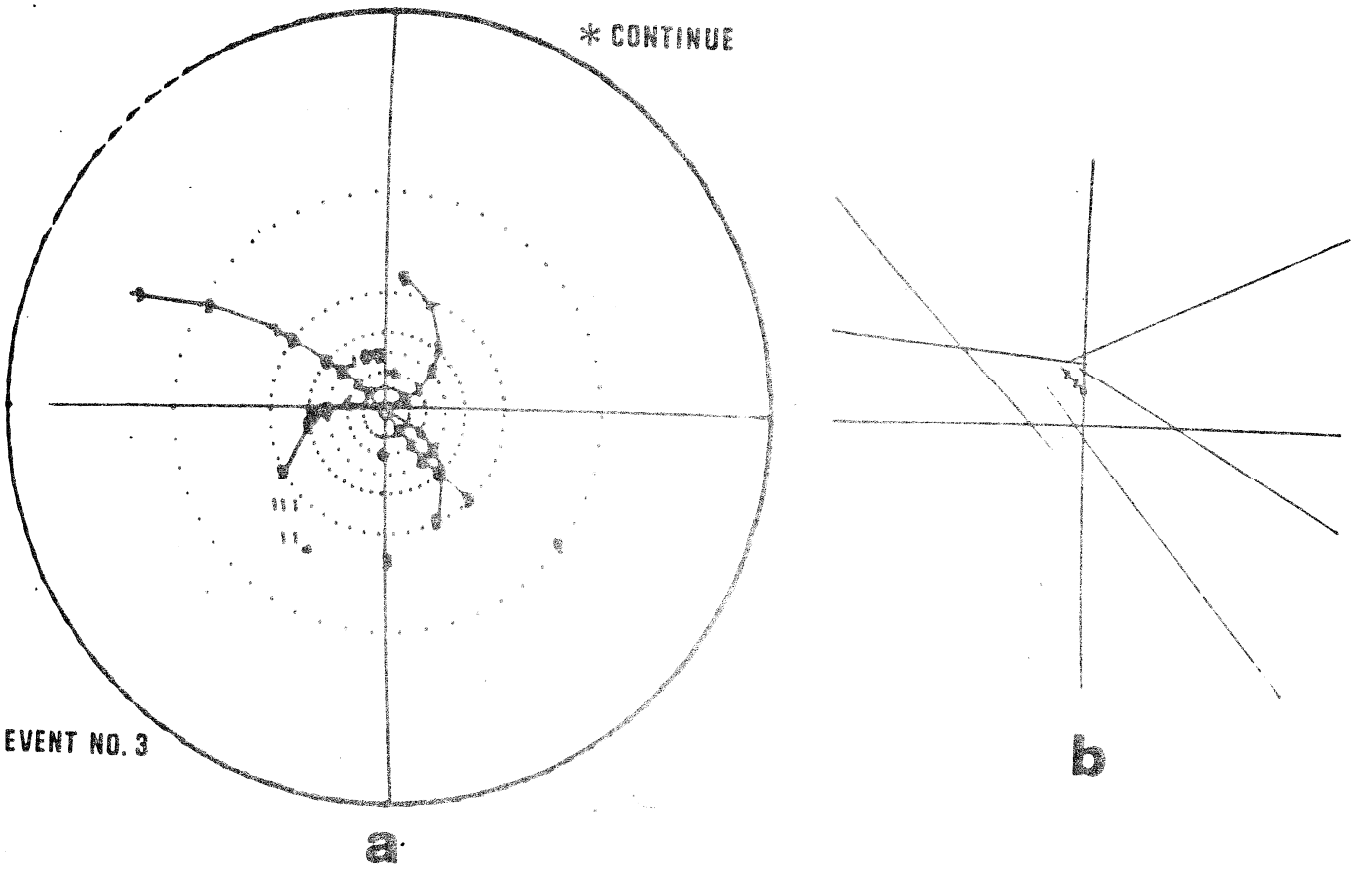

Figure 11b

Real Time Networks

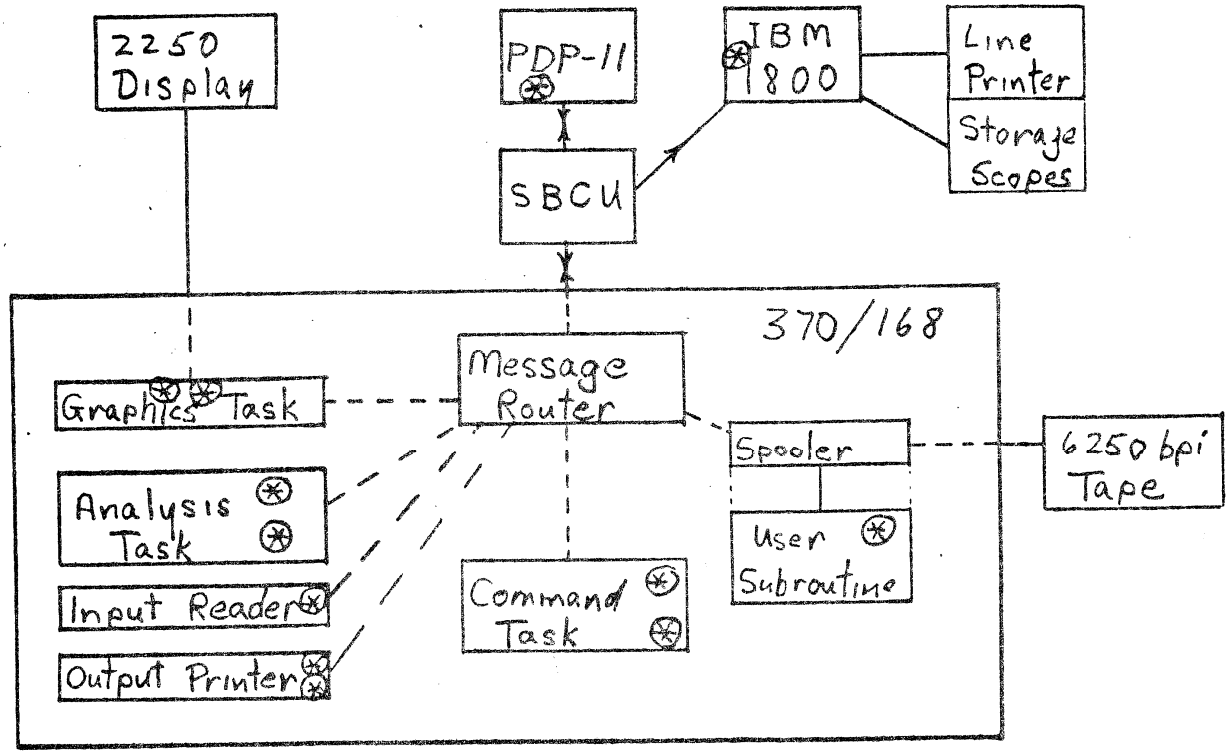

"Realistic Network" (a) ⊛ ≡ Node

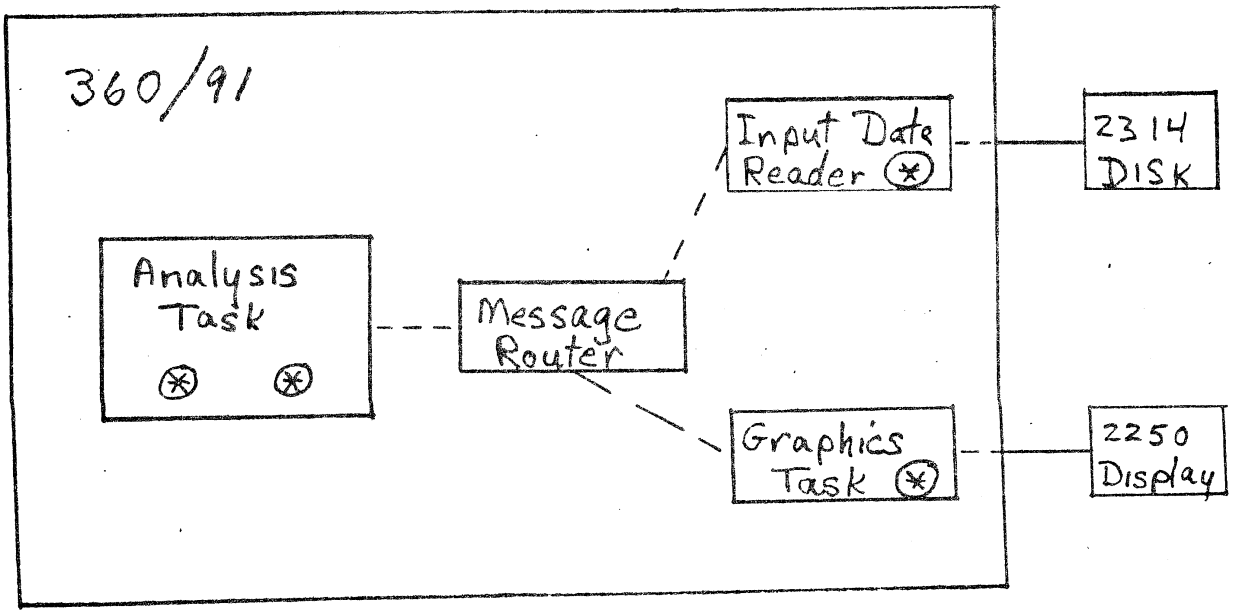

Simplified Network (b) ⊛ ≡ Node

Figure 12 - Computer Networks

August 1976

SLAC Proposal No. E-127

SUMMARY

1. Title of Experiment: Study of events with direct e^+e^- pairs in hadron collisions at 10 and 16 GeV/c.

2. Spokesmen: D.W.G.S. Leith, R. Stroynowski

Experimenters: Name	Institution
W. Dunwoodie	SLAC, Stanford University
S. Durkin	" Graduate Student
M. Ferro-Luzzi	" and CERN (leave of absence)
T. M. Fieguth	"
M. Gilchriese	" Graduate Student
A. Homma	" Graduate Student
D. Hutchinson	
W. B. Johnson	"
P. Kunz	"
T. Lasinski	"
D.W.G.S. Leith	"
J. Malos	" and Bristol University (leave of absence)
W. T. Meyer	"
B. Ratcliff	"
P. Schacht	"
S. Shapiro	"
R. Stroynowski	"
S.H. Williams	"
G. Fox	California Institute of Technology
R. Gomez	"
M. Marshall	" Graduate Student

Experimenters:	Name	Institution	
	J. Pine	SLAC	
	J. Scheid	"	
	B. Barnett	John Hopkins University	
	D. Blockus	"	Graduate Student
	C.Y. Chien	"	
	L. Madansky	"	
	A. Pevsner	"	
	C. Woody	"	Graduate Student
	R. Zdanis	"	
	R.K. Carnegie	Carleton University, Ottawa	

3. Summary

We propose a measurement of the direct e^+e^- pair production in hadronic collisions using the Large Aperture Solenoid Spectrometer (LASS). The purpose is to study the anomalous lepton/pion ratio observed in earlier experiments at low energy. The experiment will study events with e^+e^- pairs in π^-p interactions at 16 GeV/c and $\bar{p}p$, K^-p and π^-p interactions at 10 GeV/c. The equivalent of 1000 hours at 180 pps will yield ~ 7000 events with direct pairs with good mass resolution. The undistinguishable background due to Dalitz decays and external γ conversions is estimated to be ~ 30% of the signal in the low mass region ($M_{e^+e^-} < 0.3$ GeV) and ~ 2% for $M_{e^+e^-} > 0.3$ GeV. Simultaneous measurements of the associated charged hadrons will yield information on the origin of direct leptons and their production mechanism. We are ready to run in the coming accelerator cycle (October-November 1976).

4. Equipment Required for the Experiment

- LASS spectrometer, including detection system, shower counters and the on-line data acquisition system.

- 36" Liquid hydrogen target
- Existing beam line 20/21

5. Estimate of Time requirements

$\pi^- p$ at 16 GeV/c	300 hours
$\bar{p}p$ at 10 GeV/c	300 hours
$K^- p$ at 10 GeV/c	300 hours
$\pi^- p$ at 10 GeV/c	100 hours
	1000 hours

In addition we will require ~ 150 hours of low repetition rate for apparatus checks, calibration and alignment.

6. Data Analysis

a) On-line: We will require the LASS on-line computer system including the link to the 370/168 computer complex for data logging, experiment control and monitoring.

b) Off-line: The reconstruction and analysis of the data will require ~ 1000 hours of 370/168 time. An additional ~500 hours will be needed for Monte Carlo studies and for the study of single electron trigger data.